Journal Pre-proof

Proteomic investigation of interhyphal interactions between strains of *Agaricus bisporus*

Eoin O'Connor, Rebecca Owens, Sean Doyle, Aniça Amini, Helen Grogan, David A. Fitzpatrick

PII: S1878-6146(20)30031-3

DOI: https://doi.org/10.1016/j.funbio.2020.02.011

Reference: FUNBIO 1120

To appear in: *Fungal Biology*

Received Date: 20 August 2019

Revised Date: 17 February 2020

Accepted Date: 19 February 2020

Please cite this article as: O'Connor, E., Owens, R., Doyle, S., Amini, A., Grogan, H., Fitzpatrick, D.A., Proteomic investigation of interhyphal interactions between strains of *Agaricus bisporus*, *Fungal Biology*, https://doi.org/10.1016/j.funbio.2020.02.011.

Title: Proteomic investigation of interhyphal interactions between strains of *Agaricus bisporus*.

Authors: Eoin O'Connor[1,4], Rebecca Owens[1,2], Sean Doyle[1], Aniça Amini[3], Helen Grogan[4] & David A. Fitzpatrick[1,2]

Affiliations:

[1]Department of Biology, Maynooth University, Maynooth, Co. Kildare, Ireland

[2] Kathleen Lonsdale Institute for Human Health Research, Maynooth University, Maynooth, Co. Kildare, Ireland

[3] Sylvan-Somycel (ESSC - Unité 2), ZI SUD, rue Lavoisier, BP 25, 37130 Langeais, France

[4] Teagasc Food Research Centre, Ashtown, Dublin 15, D15 KN3K, Ireland

Author correspondence:

Dr. David Fitzpatrick

Genome Evolution Laboratory

Department of Biology

Maynooth University

Maynooth

Co. Kildare

Ireland.

E: david.fitzpatrick@mu.ie

T: +353-1-7086844

F: +353-1-7083845

M: +353-860681715

W: https://www.maynoothuniversity.ie/people/david-fitzpatrick

T: https://twitter.com/DFitzpatrickMU

Abstract

Hyphae of filamentous fungi undergo polar extension, bifurcation and hyphal fusion to form reticulating networks of mycelia. Hyphal fusion or anastomosis, a ubiquitous process among filamentous fungi, is a vital strategy for how fungi expand over their substrate and interact with or recognise self- and non-self hyphae of neighbouring mycelia in their environment. Morphological and genetic characterisation of anastomosis has been studied in many model fungal species, but little is known of the direct proteomic response of two interacting fungal isolates. *Agaricus bisporus*, the most widely cultivated edible mushroom crop worldwide, was used as an *in vitro* model to profile the proteomes of interacting cultures. The globally cultivated strain (A15) was paired with two distinct strains; a commercial hybrid strain and a wild isolate strain. Each co-culture presented a different interaction ranging from complete vegetative compatibility (self), lack of interactions, and antagonistic interactions. These incompatible strains are the focus of research into disease-resistance in commercial crops as the spread of intracellular pathogens, namely mycoviruses, is limited by the lack of interhyphal anastomosis. Unique proteomic responses were detected between all co-cultures. An array of cell wall modifying enzymes, plus fungal growth and morphogenesis proteins were found in significantly ($P < 0.05$) altered abundances. Nitrogen metabolism dominated in the intracellular proteome, with evidence of nitrogen starvation between competing, non-compatible cultures. Changes in key enzymes of *A. bisporus* morphogenesis were observed, particularly via increased abundance of glucanosyltransferase in competing interactions and certain chitinases in vegetative compatible interactions only. Carbohydrate-active enzyme arsenals are expanded in antagonistic interactions in *A. bisporus*. Pathways involved in carbohydrate metabolism and genetic information processing were higher in interacting cultures, most notably during self-recognition. New insights into the differential response of interacting strains of *A. bisporus* will enhance our understanding

of potential barriers to viral transmission through vegetative incompatibility. Our results suggest that a differential proteomic response occurs between *A. bisporus* at strain-level and findings from this work may guide future proteomic investigation of fungal anastomosis.

Keywords: *Agaricus bisporus*, hypha-hypha proteomics, anastomosis, hyphal-fusion, vegetative incompatibility.

List of Abbreviations

CM	Complex Multicellularity
ARP	Agaricus Resource Program
CWH	Commercial-wild hybrid
LDA	Lignin degrading auxiliary
SSDA	Statistically significant differentially abundant
Vic	Vegetative incompatibility complex
CYM	Complete yeast media
TCA	Trichloroacetic acid
DTT	Dithiothreitol
IAA	Indole-3-acetic acid
TFA	Trifluoroacetic acid
LC-MS/MS	Liquid chromatography mass spectrometry
LFQ	Label-free quantification
ORF	Open reading frame
Pfam	Protein family
KEGG	Kyoto Encyclopedia of Genes and Genomes
HMM	Hidden Markov Models
SP	Signal peptide
LSP	Leaderless-signal peptides

TM	Transmembrane membrane
NN	Neural networks
CAZy	Carbohydrate-active enzyme
Hsp	Heat-shock protein
GMC	Glucose-methanol-choline
NDGS	NADPH-dependant glutamate synthase
GH	Glycosyl hydrolase
ROS	Reactive oxygen species

1. Introduction

Unicellular fungi from the Ascomycota phylum, such as the yeasts *Candida albicans* and *Saccharomyces cerevisiae*, form adhesions for cell-cell communication, biofilm formation, pathogenesis, commensalisms and primary phases of saprophytic interactions composed of mannoproteins covalently bound to the cell wall (Lipke, 2018). Adhesion and signalling domains are critical for the innovation from unicellularity to complex multicellularity (CM). Phylogenomic and genomic evidence suggests that CM has independently evolved in five eukaryotic groups including the fungi (Knoll, 2011). Within the fungi it occurs in most major clades and displays at least 8 and perhaps as many as 11 independent origins (Nagy et al., 2018). A variety of complex micropore structures bridge intracellular connections of multicellular ascomycete and basidiomycete hyphae (Markham, 1994). Hyphae are the structural units, segmented by septa (Harris, 2001), of vegetative growth in filamentous fungi. They are tubular in shape and have polarised extensions through apical growth mediated by high pressure and vesical transport of a multitude of important enzymes for cell wall biosynthesis. These enzymes remain inactive in cytoplasmic transit until buried in the transmembrane of apical regions, whereby the synthesis of β-1-3-glucan and chitin can occur and recruitment of cytosolic-derived glycoproteins from the endoplasmic reticulum-to-Golgi pathway for cell wall biogenesis (Riquelme *et al*., 2016). In fast growing hyphal tips, a cytoskeletal-derived structure known as the Spitzenkörper, both fuses and extends the cell wall of the apex by recruitment of transport vesicles (Bartnicki-Garcia *et al*., 1989) and is responsible for the directionality of hyphal growth (Reynaga-Pena et al., 1997). Hyphae both extend at their apex and form sub-apical growth of branching hyphae commonly in a bifurcating fashion (Girbardt, 1957, 1969; Lopez-Franco and Bracker, 1996; Riquelme and Bartnicki-Garcia, 2004). Anastomosis (hyphal fusion) of branching and apical hyphae takes place to form the reticulating network architecture known as the mycelium (**Figure 1**).

The process of anastomosis allows the mycelium to form large single-unit colonies for purposes of heightening exocytosis coverage for chemotactic activity and hydrolysing proteins allowing for physical expansions in ecosystems. Mating of combinations of different cultures was first evaluated when it was found that mixing cultures of the model fungus *Aspergillus nidulans* created parasexual recombinants (Pontecorvo *et al*., 1953). Parasexuality in filamentous fungi allows heterokaryons with different genotypes to undergo anastomosis and form a new hybrid heterokaryotic mycelium with cytoplasmic exchange (plasmogamy) and novel nuclear types, conferring genetic advantages to species, particularly those that may have low rates of meiosis or recombination (Glass and Fleissner, 2006; Pontecorvo, 1956; Swart et al., 2001). To prevent anastomoses of incompatible hyphae or hyphae that may incur deleterious interactions, a vegetative incompatibility complex (*vic*) and a sexual incompatibility (*het*) system, mediated by mating loci, are found in filamentous fungi. Incompatible fusions of fungal hyphae can trigger inhibited growth and even programmed cell death (Biella et al., 2002; Garnjobst and Wilson, 1956; Labarere and Bernet, 1977; Sarkar, 2002). These systems can act as protective mechanisms where anastomosis with non-self hyphae could be disadvantageous. An example of such is fusion with a foreign mycelium harbouring infectious intracellular mycoviruses (Chu et al., 2002; Grogan et al., 2004; Kashif et al., 2019; Romaine et al., 1993; van Diepeningen et al., 1998).

Agaricus bisporus is the most extensively cultivated mushroom in the world and is grown commercially on a pasteurised compost substrate most commonly composed of wheat straw, horse and/or poultry manure and gypsum (Van Griensven, 1987; Vedder, 1978). In commercial practice, two main phases precede the formation of mushrooms; the spawn run phase and casing phase. Focusing on the former, the success of the spawn run phase is dependent on the compost substrate being heavily colonised by *A. bisporus* hyphae (Kabel et al., 2017), a process that involves mass breakdown of aromatic lignins, cellulose,

hemicellulose and nitrogen sources (including bacterivorous nutrient acquisition (Fermor et al., 1991)). To begin this process, pasteurised compost is 'seeded' with *A. bisporus*-coated spawn grains that instigates the process of compost colonisation. These isolated colonies must undergo self-recognition and anastomose with other colonies. While studies have focused on molecular mechanisms governing how *A. bisporus* breaks down commercial compost (Pontes et al., 2018; Wood and Thurston, 1991; Yague et al., 1997), little attention has been paid to the impact of colony recognition/anastomosis in this process. To address this, we have analysed the proteomic response of three different strains of *A. bisporus in-vitro* to build an understanding of the molecular mechanisms governing inter-hyphal interactions. Particular focus is paid to the globally cultivated present day white-hybrid mushroom strains, as they have been almost exclusively used in commercial mushroom industries for nearly three decades due to their commercial appeal. There is very little genetic variation with these white-hybrid strains (Sonnenberg et al, 2017), so they are all susceptible to the same diseases worldwide, including disease-causing mycoviruses, the transmission of which is governed by anastomosis of infected mycelium with healthy mycelium (Grogan et al., 2003). Breeding research that focuses attention on novel hybrids that have vegetative incompatibility with present day white-hybrids, and which do not readily form hyphal fusions, would pave the way for 'virus-resistant' varieties. This is exemplified by a control method once used against mushroom virus disease, which required growing a "virus-breaker" strain such as *A. bitorquis*, instead of *A. bisporus*, as they do not readily anastomose, thereby preventing transmission of mycoviruses to the new crop (Van Zayen 1978;Fletcher and Gaze, 2007), although hyphal anastomoses between them may still occur. Three *A. bisporus* are included in this study which include a present day white hybrid Sylvan A15, a novel experimental hybrid strain between a commercial white and a wild brown strain, referred herein as CWH, which has shown heightened resistance to mushroom virus X (data unpublished) and ARP23,

a wild isolate of the ARP collection (Callac et al., 1996). Wild strains of *A. bisporus* have also shown promise in terms of disease resistance (Glass et al., 2000; Glass and Kuldau, 1992; Leslie, 1993) due to their lack of vegetative compatibility (in heterokaryotic terms) with commercial white strains.

Inter-hyphal fusion in the commercial button mushroom fungus *A. bisporus* is a key area of interest due to its importance in successful compost substrate colonisation and the roles it plays in the spread of deleterious mycoviral diseases. In this study, phenotypic evidence shows A15 anastomoses more readily with itself than with CWH or ARP23 strains. By using a combination of three distinct strains of *A. bisporus*, an untargeted approach was taken to elucidate the proteomic response of anastomosis.

2. Methods

2.1 Strains and culture conditions

Three strains of *A. bisporus* were used in this study: (1) commercial strain A15, (2) a novel experimental hybrid strain CWH from a cross between a commercial white and a wild-type brown, and (3) a wild strain ARP23 from the *Agaricus* Resource Program (ARP) collection (Callac et al., 1996), all obtained from Sylvan Inc., France. All strains were grown on complete yeast media (CYM) containing 2 g proteose peptone, 2 g yeast extract, 20 g glucose, 0.5 g $MgSO_4$, 0.46 g KH_2PO_4, 1 g K_2HPO_4, 10 g agar in 500 ml dH_20. Once molten media had solidified and cooled, a sterile sheet of cellophane, the same circumference as the petri dish was added to the surface of the CYM. CYM was either inoculated with a single agar plug for monoculture preparations or two agar plugs placed either end of the petri dish for co-culture preparations. Cultures were grown for two weeks in the dark, at 25 ºC. Two weeks allows enough time for ample hyphal interaction of co-cultures. The following samples were prepared: monocultures of A15, CWH and ARP23; co-cultures of A15-A15, A15-CWH and A15-ARP23.

2.2 Extracellular and secreted protein extraction

Equal numbers of monocultures (n=8) to co-cultures were used to minimize quantity bias of starting materials for any particular strain. The entire mycelial mass was subject to protein isolation, as opposed to targeting growing edges of monocultures or growing edge and interaction zones of co-cultures, so as to capture the broadest suite of secreted and extracellular proteins present. Cellophane coated with fungal hyphae was carefully removed with sterile forceps and added to 50 ml 50 mM potassium phosphate pH 7.5, 1 µg/ml Pepstatin A, 1 mM PMSF, 1 mM EDTA to allow for detachment of the mycelial sheet from

the cellophane. Mycelium/buffer mix was gently agitated for 24 h on a daisywheel at 4°C. Hyphal suspensions were filtered through Miracloth and filtrates were clarified by centrifuging at 25,000 x g for 30 min (4°C), twice. Supernatants were brought to 15% (v/v) trichloroacetic acid (TCA) using 100% TCA. TCA suspensions were agitated overnight using a daisywheel (4°C). Protein precipitate was centrifuged at 1700 x g for 45 min (4°C) and pellets were washed with 20% (v/v) 50 mM Tris-base in acetone with two additional Tris-buffered acetone washes and one additional acetone wash. Dried-protein pellets were resuspended in 6 M urea, 2 M thiourea and 100 mM Tris-HCl pH 8.0. Protein concentrations were calculated using the Qubit Protein assay kit (ThermoFisher, Waltham, Massachusetts, USA), measurements were performed using the Qubit Fluorometer 1.0 (ThermoFisher, Waltham, Massachusetts, USA) and resuspended protein concentrations were normalised for each sample. Urea concentration was adjusted to 1 M by addition of 50 mM ammonium bicarbonate. Proteins were reduced and alkylated by addition of 0.5 M DTT and 0.55 M IAA, with an incubation for 15 min in the dark at room temperature (Collins et al., 2013). Protein digestion was performed using ProteaseMAX at a concentration of 0.01% (w/v) followed by addition of sequencing-grade trypsin. Tryptic peptides were acidified with trifluoroacetic acid (TFA) and desalted using C_{18} Ziptips (Millipore® Ziptips C18) (O'Keeffe et al., 2014; Owens et al., 2015; Sipos et al., 2017).

2.3 LC-MS/MS analysis of *A. bisporus* proteins

LC-MS/MS identification of *A. bisporus* proteins was carried out on tryptic peptide mixtures using a Q-Exactive (ThermoFisher Scientific, U.S.A) coupled to a Dionex RSLCnano. LC gradients from 3-45% were run over 2 h and data were collected using a Top15 method for MS/MS scans. Spectra were analysed using the predicted protein databases of *Agaricus bisporus* var. *bisporus* (H97) v2.0 (Morin et al., 2012) for the main protein data set and functional analyses. Spectra were also analysed against the predicted proteome of

Agaricus bisporus var. *bisporus* ARP23 (O'Connor *et al.*, 2019) for the analysis of ARP23 specific hits. This was done by concatenating the H97 and ARP23 genomes and considering protein hits to the ARP23 genome alone. MaxQuant (version 1.6.2.3) with integrated Andromeda was used for database searching (Cox and Mann, 2008). MaxQuant parameters were as previously described (Owens et al., 2015). Removal of reverse hits and contaminant sequences, filtering of protein hits found in only a single replicate (n = 3), and Log_2 transformation of LFQ intensities was performed using Perseus (version 1.4.1.3; (Tyanova et al., 2016)).

2.4 Bioinformatics analyses

Peptides mapped to translated open reading frames (ORFs) in the genome of *A. bisporus* var. *bisporus* (H97) (Morin et al., 2012) were functionally annotated with known protein family (Pfam) domains and domains allocated from the Interpro consortium using InterproScan 5 (Jones *et al.*, 2014). Gene ontology (GO; Ashburner *et al.*, 2000) IDs were assigned with Interoscan5 and a term map generated for functional descriptions with the Yeastmine resource (Balakrishnan et al., 2012). The proteomes of monocultures and co-cultures were analysed using KEGG (Kyoto Encyclopaedia of Genes and Genomes; Ogata *et al.*, 1999) with pathway annotations assigned by BlastKOALA (Kanehisa *et al*., 2016). Putatively secreted proteins were located with SignalP v3 (Dyrløv Bendtsen et al., 2004). SignalP v3 was chosen over newer versions (v4 and v5) as studies have established it is an effective prediction tool for fungal secretomes (Sperschneider et al., 2015). Criteria for putatively secreted proteins in SignalP v3 were as follows; NN D score of ≥0.5, HMM S probability value of ≥0.9 and NN Y_{max} score of ≥0.5. TMHMM was used to predict transmembrane (TM) domains (Sonnhammer *et al*., 1998). Proteins containing TM domains after the signal peptide (SP) cleavage site are embedded in the membrane and so normally TMHMM is used as a filtering tool to remove proteins that are not secreted into extracellular

space (Käll *et al*., 2007). However, as these proteins may be embedded in the outer membrane of cells, they were not removed for the purposes of this study. SecretomeP was also used to predict leaderless signal peptides (LSPs) of secreted proteins that do not contain classical SignalP domains (Bendtsen *et al.*, 2004). A cut-off of NN-score/SecP ≥0.6 was applied.

Comparative quantitative proteomics was carried out through particular focus on proteins which were statistically significant differentially abundant (SSDA; $P < 0.05$, fold change ≥ 1.5) between pairwise comparisons of samples. Each monoculture and co-culture proteome was searched against the dbCAN2 (Zhang et al., 2018) to identify Carbohydrate Active Enzymes (CAZys; Cantarel *et al.*, 2009). All gene accession IDs listed in this text are preceded by the Joint Genome Institute (JGI) identifier 'jgi|Agabi_varbisH97_2'.

3. Results

3.1 Interactions of three strains of *A. bisporus*

Observations were made between anastomoses of A15 with A15 (A15-A15), A15 with CWH (A15-CWH) and A15 with ARP23 (A15-ARP23). A clear distinction was evident between the interactions of A15-A15 (self) and the other combinations. When A15 was paired with itself, a plethora of hypha-hypha fusion ensued upon interaction of the two colonies growing in the same trajectory (positive tropism) (**Figure 2A**). However, a characteristic demarcation zone of interaction was still evident pertaining to a level of recognition between cultures from different sources. The interaction of A15 with CWH was less prominent, with a distinct zone where hyphal extension was halted (negative tropism) and evidence of hyphal fusion between colonies was only observed microscopically (data not shown) (**Figure 2B**). Although there was clear interaction between A15 and ARP23, a defined barrier of interaction was established between the two colonies (combination of positive and negative tropism) (**Figure 2C**).

3.2 Monoculture and co-culture proteomes

The total number of unique unambiguously-detected proteins, for all monoculture and co-culture comparisons, was 1,500 when aligned to the predicted proteome of *A. bisporus* (H97; commercial cultivar) and 1,510 when aligned to the predicted proteome of *A. bisporus* (ARP23; wild strain). By concatenating the two genomes a total number of 1,828 proteins were detected, indicating that certain proteins were uniquely identified or absent in the concomitant strain genomes (see **Table_S1**).

Qualitative and quantitative data for the whole proteome (putatively secreted proteins and also proteins found extracellularly) were combined to assess the proteomic response of anastomosing strains versus axenic cultures (**Figure 3)**. KEGG analyses revealed key differences in the pathways of proteomes between monoculture and co-cultures (**Figure 4**). Relative to monocultures, higher levels of carbohydrate metabolism and genetic information processing were found in all three co-cultures. Interestingly, the A15-A15 co-culture displayed the greatest levels of carbohydrate metabolism and genetic information processing with the A15-CWH co-culture having the lowest levels (**Figure 4**).

3.3 Changes in the secreted proteome during anastomosis

The total number of proteins predicted to be secreted was 337. A total of 463 proteins were SSDA when all treatments were considered (**Table_S2**) and 247 of these were non-redundant (**Table_S2**). Putatively secreted proteins with significantly differential abundances were assessed for their possible roles in fungal anastomosis.

Glucose-methanol-choline (GMC) oxidoreductase (accession:205329) exhibited increased abundance in most co-cultures compared to monoculture preparations (**Figure 5 & Table_S2**). An interesting pattern was observed, where the levels of GMC oxidoreductase were higher in A15-CWH to A15 (log_2 5.41-fold) than to A15-CWH to CWH pairwise comparisons (**Figure 5)**. The same pattern was evident in A15-ARP23 to A15 (log_2 3.47-fold) and A15-ARP23 to ARP23 comparisons (**Table_S2**). Our results also showed that a shikimate kinase (accession:210736) showed increased abundance in A15-A15 to A15 (log_2 3.47-fold) and A15-ARP23 to ARP23 (log_2 3.88-fold) comparisons (**Figure 5 & Table_S2**).

Proteins implicated in the stress-response including a hydrophobin (accession:138066) displayed increased abundance (log_2 3.25-fold) when comparing A15-

ARP23 to A15 cultures (**Figure 5** & **Table_S2**). This hydrophobin was also increased in abundance in the A15-A15 to A15 comparison (log_2 3.25-fold; **Table_S2**)

Interestingly the culture comparisons of ARP23 to A15-ARP23 displayed increased levels of a protein (log_2 1.67-fold, accession:189493) relating to the *het* system (*het*erokaryon incompatibility; Glass and Kuldau, 1992). Het-C plays a role in the recognition of self and non-self (Wu et al., 1998).

3.4 Changes in the extracellular (non-secreted) proteome during anastomosis

Of the 1,510 proteins we located, 1,173 did not contain a signal peptide, atypical signal peptides or LSPs and were therefore considered not to be secreted. These proteins were investigated however as they were extracellular and may also play key roles in inter-hyphal interactions. One non-secreted protein of interest included Profilin (**Table_S3**, accession:77709). Profilin was observed in greater amounts in all A15 co-cultures (A15-A15 log_2 2.18-fold, A15-CWH log_2 2.56-fold & A15-ARP23 log_2 1.80-fold).

Another non-secreted protein of interest was Glucanosyltransferase (**Figure 5**, **Table _S3**, accession:189849). Elevated levels of abundance for this protein were observed when comparing A15-A15 to A15 (log_2 2.83-fold) and A15-CWH to A15 (log_2 3.15-fold) cultures (**Figure 5 & Table_S3**). In contrast, the inverse was observed for the A15-CWH to CWH comparison where reduced abundance was observed (log_2 -3.03-fold change).

Our proteomic analyses support the observation that the A15 and ARP23 pairing creates biotic stress due to the high abundance of heat-shock protein 70 (Hsp70) in both culture comparisons of A15-ARP23 to A15 and A15-ARP23 to ARP23 (**Figure 5 & Table_S3,** accession:195173). A Hsp90 ATPase (accession: 63138) was also observed in similar patterns to Hsp70 in the A15-ARP23 to A15 and A15-ARP23 to ARP23 comparison with an additional finding of reduced abundance in the A15-CWH to CWH comparison (log_2

-4.71-fold; **Table_S3**). Another protein observed to significantly increase in abundance was a laccase-5 (Pfam description as multi-copper oxidase, accession:135711) which is elevated in both A15-ARP23 to A15 (log_2 3.09-fold) and A15-AP23 to ARP23 (log_2 2.17-fold) culture comparisons (**Figure 5 & Table_S3**).

When comparing the extracellular proteomes of A15 co-cultures versus A15, a NADPH-dependant glutamate synthase (NDGS) (accession:176670) showed increased abundance in all three comparisons (log_2 8.22-fold, log_2 7.98-fold & log_2 7.21-fold respectively) and also accounted for the largest fold change observed (**Table_S3**). NDGS are involved in nitrogen metabolism. Another protein related to nitrogen metabolism observed at significantly increased abundance in all three comparisons was urease (**Table_S3** accession:183828). Increased urease abundance was the highest in A15-ARP23 to ARP23 comparisons (log_2 6.0-fold) and increased abundance was also observed in all A15 co-cultures versus A15 (**Table_S3**).

3.5 Secreted and extracellular proteins of carbohydrate metabolism in comparisons of A15 monocultures to A15 co-cultures

Proteins relating to carbohydrate metabolism were examined between A15 monocultures and the three A15 co-culture interactions (**Table 2)**. Overall, a pattern of reduced levels of carbohydrate-active SSDA proteins was observed in anastomosing cultures when compared to individual constituent monocultures, regardless of the levels of vegetative compatibility observed (**Table 2**).

Levels of cellulase (accession:229390) were significantly lower in anastomosing cultures of A15-15, A15-CWH and A15-ARP23 (log_2 -6.67-fold, log_2 -5.78-fold and -6.79-fold, respectively; **Table 2**). β-Glucanase (GH16, accession:194297) levels were not significantly differentially abundant in either A15-A15 or A15-CWH cultures, but were

increased (log_2 1.86-fold) in the A15-ARP23 culture (**Table 2**). A polysaccharide deacetylases (PD, accession:114473) displayed increased abundance in all three comparisons while a second PD (accession: 194656) displayed significantly increased abundance in the A15-A15 and A15-CWH comparisons (**Table 2**). A BLASTP database search against the NR database of GenBank for both proteins showed the closest hit outside of the *Agaricus* genus is to a chitin deacetylase from *Leucoagaricus sp. SymC.cos* (Query cover: 69%, Identity: 67.85%).

Another enzyme of interest is β-*N*-acetylhexosaminidase (GH20 accession:193587). Levels of GH20 were found to be significantly increased in the A15-A15 co-culture (log_2 1.51-fold) and reduced in A15-CWH and A15-ARP23 cultures (log_2 -2.42-fold and log_2 -2.00-fold respectively).

Distinct differences between the CAZyme arsenals of monocultures versus A15 co-cultures (**Figure 6A**) were observed. Monocultures had a similar array of CAZymes with evidence for 94, 92 & 94 proteins for A15, CWH and ARP23 monocultures respectively. Furthermore, 41 unique proteins were observed in all three monocultures (**Table_S4**).

Comparing co-cultures, there is evidence for 68, 72 and 127 CAZymes for A15-A15, A15-CWH and A15-ARP23 co-cultures with 46 unique proteins observed in all three co-cultures (**Table_S4)**. The higher number of CAZymes in the antagonistic interaction between A15-ARP23 suggests that the diversity of CAZymes is increased in incompatible interactions (**Figure 2C**) . In terms of individual CAZymes classes, the largest expansion observed is for LDA enzymes in the A15-ARP23 co-culture (n=24, **Figure 6A**). Furthermore, A15-A15 shows a drop in LDA enzymes in co-culture (n = 8) compared to A15 monoculture (n = 15). The accumulation of reactive oxygen species (ROS) is attributed with contact zones of antagonistic interactions between fungi and high levels of oxidative stress (Silar, 2005).

Figure 6A suggests that regulation of LDA enzymes is considerably altered in the compatible and incompatible interactions. **Figure 6C** shows that the expansions in different CAZyme classes in A15-ARP23 are not simply a consequence of the two different strains having distinct enzymatic arsenals, as their monoculture CAZyme profiles indicate no unique CAZys are found (no addition of unique CAZymes). Specific CAZymes in A15-CWH co-cultures are the lowest (n = 5; **Figure 6B**). Pectinase was detected in all monocultures but was found only in the A15-ARP23 co-culture (**Figure 6A**). Production of cellulase and hemicellulose enzymes tended to be highest in the ARP23 monoculture and co-cultures (**Figure 6A**).

3.6 Unique co-culture proteomic profiles

Comparisons of SSDA proteins were made between the three co-cultures to decipher if the three different interactions induced a distinct proteomic response relative to A15 monocultures (**Figure 7**). Overall 294 unique SSDA proteins were observed across all three co-cultures. Of these, 95 proteins were common to all three interactions and 62 of them showed increased abundance while the remaining 33 showed a significant decrease in abundance. The A15-A15 and A15-CWH co-cultures shared the greatest number of unique proteins between two co-cultures (n = 71) (**Figure 7)**. The A15-ARP23 interaction was the most distinct interaction sharing relatively low number of proteins in pairwise-comparisons (10 with A15-A15 & 17 with A15-CWH) and also having the greatest number of unique strain specific proteins overall (n = 43). Three putative laccases (accessions: 135711, 139148 & 184981) were found as SSDA only in A15-ARP23 co-culture (**Table_S5)**. Proteins involved in polarised growth of hyphae including a septin (accession:192322) and oxysterol-binding protein (accession: 195179) were found exclusively in A15-A15 (**Table_S5)**.

4. Discussion

Many studies into the outcomes of fungal interactions and anastomosis have been carried out in the ascomycetes and basidiomycetes, ranging from biocontrol of economically-damaging plant pathogens to understanding wood decomposition fungal community structures (Ainsworth and Rayner 1986; Boddy, 2000; Van Bael *et al.*, 2009; Schöneberg *et al.*, 2015; El Ariebi *et al.*, 2016; Hiscox *et al.*, 2017). Many studies have also been conducted into the hyphal fusion process fungi undertake to form mycelium (as reviewed by (Glass, 2004)) and the genes that govern recognition processes mitigating anastomosis (Smith *et al.*, 2006). To our knowledge, only one other study examining the proteomic response of antagonistic white rot fungi *in vitro* has been undertaken to date (Zhong et al., 2018) and no study aimed specifically at the proteomic response during the process of anastomosis in a range of vegetative compatibilities has been performed. Our use of three different strains of *A. bisporus* is an effective model to study such a response for the following reasons 1) They are conspecific and so interactions will represent a more conserved system of recognition and interaction compared to a study that focuses on different species of fungi. 2) anastomosis is a key element of the mushroom growth process, and virus transmission. 3) the three strains display a distinct variety of interactions from full vegetative compatibility (A15-A15), lack of interaction of receding/repelling cultures (A15-CWH), and levels of vegetative incompatibility (A15-ARP23) (**Figure 2**). This lack of interaction therefore confirms the use of strains CWH and ARP23 as virus-breaking varieties.

Anastomosis is a crucial process in fungi regarding substrate colonisation, nutrition acquisition, hyphae morphogenesis, and recognition between neighbouring mycelia.

Outcomes of gene-regulation reflected in the comparisons of protein profiles in the extracellular/secreted proteomes during the process of anastomosis were elucidated. A15 dominated the experimental setup and subsequent data analysis as the primary dual-culture partner (**Figure 2**). The rationale for this is that A15 represents present-day white hybrids while CWH and ARP23 represent good dual-culture partners in terms of understanding the basis of vegetative incompatibility. For the purpose of this investigation, the methods used to extract proteins were tailored to extracellular and secreted protein acquisition from hyphae to minimise cell lysis. However, extracellular proteins with no evidence of being actively secreted (i.e. lacking signal peptide) were also considered as they may also play key roles in inter-hyphal interactions, due to the fact that the process from recognition to anastomosis can often result in levels of cell lysis (via apoptosis) and necrosis leading to the release of cytosolic proteins into extracellular spaces (Bourges et al., 1998; Paoletti and Clavé, 2007). As very little is known of the proteomic mechanisms governing anastomosis, lists of up- and down-regulated proteins were separated into potentially important proteins involved in anastomosis (**Figure 5**) and carbohydrate metabolism (**Table 2**). The total number of unique unambiguously-detected proteins, for all monoculture and co-culture comparisons, was ~1,500 when individually aligned to the predicted proteome of *A. bisporus* H97 (1,500) or ARP23 (1,510). Concatenating the two proteomes into a single proteome database resulted in a total number of 1,828 detected proteins. Therefore, certain proteins were uniquely identified or absent in the concomitant strain genomes. This is unsurprising as pangenome analyses of *A. bisporus* strains have shown high levels of gene variability between individual strains (O'Connor et al., 2019).

Proteins were classified as secreted if they contained a signal peptide (SignalP v.3). Proteins with a signal peptide and transmembrane domain were considered as putatively secreted as they may represent proteins on cellular surfaces that play a role in inter-hyphal

contact. Similarly, proteins containing atypical signal peptides or LSPs were also considered secreted. The total number of proteins predicted to be secreted was 337 and 247 of these were SSDA (**Table_S2**). SSDA proteins that may have a role in fungal anastomosis were examined. Our results showed that GMC oxidoreductase exhibited increased abundance in most co-cultures. GMC oxidoreductase forms a diverse family of lignin-degrading auxiliary (LDA) enzymes and contains a signature flavin adenine dinucleotide (FAD) cofactor. Extracellular H_2O_2 is produced by GMC oxidoreductase and used as the overall oxidiser of lignin and polysaccharides in brown- and white-rot fungi (Ferreira et al., 2015). Our results also showed that a shikimate kinase showed increased abundance in A15-A15 to A15 and A15-ARP23 to ARP23 comparisons (**Figure 5 & Table_S2**). The shikimate pathway has a multitude of functions but primarily forms the crossover from metabolism of carbohydrates to the biosynthesis of aromatic compounds (Herrmann and Weaver, 1999).

An important step preceding mushroom formation is the substrate-colonisation phase during the spawn-run phase, whereby *A. bisporus* mycelium colonises and derives nutrition from the complex, nutrient-rich ligno-cellulosic mushroom substrate. Mycelium growth throughout the substrate involves anastomosis en masse, as isolated colonies begin to come into contact. Proteins relevant to carbohydrate metabolism can be involved in the restructuring of self or non-self hyphae architectures and therefore, were considered as possible players in the process of anastomosis and not solely for nutrient acquisition (Cabib, 2009; Ragni et al., 2007). Previous work has shown that cellulose is degraded during mycelial growth and levels of endocellulase peak during periods of fruitification in *A. bisporus* (Claydon et al., 1988; Manning and Wood, 1984). In our analysis, levels of cellulase were significantly lower in anastomosing cultures of A15-15, A15-CWH and A15-ARP23 (**Table 2**). Proteins which may not necessarily directly contribute to anastomosis may still be relevant to the competition for substrate between two neighbouring mycelia. The more

obvious candidates warranting examination for this study were proteins involved in biosynthesis of hyphal components and polymerisation of the cell wall. After refining our proteomic datasets through statistical significance tests and cut-offs in minimum relative abundances, many key proteins involved in hyphal morphogenesis were still highly represented in the interaction cultures (**Table 2**), including profilin, glucanosyltransferase, and glycosyl transferase 1. For example, profilin was observed in increased abundance in all A15 co-cultures relative to A15 monoculture. Profilin has high affinity for actin and replaces ADP for ATP in G-actin resulting in a profilin-ATP-actin complex that accelerates rates of actin filament elongation and nucleation (Babich *et al.*, 1996; Kovar *et al.*, 2006; Rangamani *et al*., 2014). Similarly, elevated levels of abundance for glucanosyltransferase were observed when comparing A15-A15 to A15 and A15-CWH to A15 cultures (**Figure 5 & Table_S3**) Glucanosyltransferase has known functions in cell wall expansion and hyphal growth by the splitting of β-1-3-glucan and joining of the newly exposed reducing end to the non-reducing end of another β-1-3-glucan (Hartland et al., 1996) and therefore has a pivotal role in apical growth and morphogenesis (Saporito-Irwin et al., 1995). Increased abundance could possibly be an indication of the competition for hyphal growth when paired with a neighbouring mycelium. In contrast, reduced abundance of glucanosyltransferase was observed for the A15-CWH to CWH comparison suggesting that CWH may repress the growth of hyphae in the presence of A15. Furthermore a fundamental enzyme in the process of cell wall formation through the rearrangement of 1,3-β-glucanase is glycosyl transferase family 1. The relative abundance of this enzyme increased for all A15 co-cultures (**Table_S3**).

Our results highlight changes in abundances of proteins involved in nitrogen metabolism. NADPH-dependant glutamate synthase (NDGS) showed increased abundance in all co-culture comparisons (**Table_S3)**. NDGS are broadly involved in housekeeping functions through activities in nitrogen metabolism by catalysing the assimilation of

ammonia into glutamine and glutamate (Ahmad and Hellebust, 1991). Some studies hypothesise that NDGS plays a role in bridging a connection in carbohydrate and nitrogen metabolism in yeast, the former acting as a producer of energy and the latter for biomass production by means of cytosol and mitochondria shuttling (Guillamon *et al.*, 2001), just as in other known redox shuttles in yeast (Bakker, 2001). Another protein related to nitrogen metabolism that was observed at significantly increased abundance in all comparisons was urease. This is a nickel-containing enzyme associated with breakdown of urea. Urea is found in high concentrations in *A. bisporus* fruit-bodies, particularly the primordia (Wagemaker et al., 2006). The increase in urease abundance may reflect the use of internal urea as a nitrogen source for generating energy for hyphal growth (Baars et al., 1994; Mobley and Hausinger, 1989) or may be evidence of nitrogen starvation by classical nitrogen assimilation means as urease enzymes have been shown to be induced in times of nitrogen starvation (Beckers et al., 2004).

The vegetative-compatible interaction (A15-A15 **Figure 2A**) showed the greatest increase in abundance for hyphae remodelling proteins such as profilin and β-*N*-acetylhexosaminidase. β-*N*-acetylhexosaminidase is a chitinase involved in the degradation of chitin by hydrolysis of N-acetyl-hexosaminyl residues. Chitinases are also known for their roles in hyphal growth by remodelling the cell wall during horizontal growth (Takaya *et al.*, 1998; Takaya *et al.*, 2005). Putative chitin deacetylases also show increased abundance in all three co-cultures (**Table 2**). Intracellular chitin deacetylase has been implicated in cell wall formation in *Mucor rouxii* (Davis and Bartnicki-Garcia, 1984) while extracellular/secreted chitin deacetylases are known for their roles in pathogenicity of *Colletotrichum lindemuthianum* through aiding in evasion of host plant immunity by modifications of chitin on penetrating hyphae (Tsigos and Bouriotis, 1995). Increased abundance of the levels of glycosyl transferase 1, which is involved in hyphal extension, were high in all A15 co-

cultures regardless of the interaction partner (**Table_S3**). Furthermore, a septin and oxysterol-binding protein were found exclusively in A15-A15 (**Table_S5)**. Septins are involved in polarised growth of hyphae by acting as a scaffold during fungal morphogenesis (Khan *et al*., 2015) and oxysterol-binding proteins are implicated in vesicular-trafficking among other functions (Raychaudhuri and Prinz, 2010). These are examples of proteins that may be beneficial in an interaction where anastomosis is advantageous to the neighbouring mycelia, such as that in A15-A15. The A15-A15 co-culture displayed the greatest levels of carbohydrate metabolism and genetic information processing which may be indicative of a vegetative-compatible interaction (**Figure 4**), conversely the A15-CWH co-culture displayed corresponding low levels and may be indicative of the lack of interaction evident between A15 and CWH (**Figure 2B**).

The interaction of A15-ARP23 showed signs of biotic stress. A15 formed hyphal plumes of aerial growth in every interaction replicate with ARP23 (**Figure 2C**). Aerial or 'fluffy' growth of mycelium *in vitro* can be an indication of stress (Beites et al., 2015; Flärdh and Buttner, 2009; Hansberg and Aguirre, 1990). Aerial growth occurs as polar extension of apical hyphae attempt non-planar growth from the current substrate surface to a new area. Our proteomic analyses reinforced this phenotype as we observed increased abundance of secreted stress-response associated proteins Hsp70 and Hsp90 ATPase (**Figure 5**). Hsp70 protects against aberrant aggregation of proteins by binding to hydrophobic residues of proteins partially unfolded by thermal or oxidative stress (Mogk et al., 2003). It has been shown that Hsp70 has known functions in translation by assisting nascent polypeptides through ribosomal channels (Nelson et al., 1992). The combination of Hsp70 and Hsp90 play important roles in fungal morphogenesis (Tiwari *et al*., 2015). Hsp90 did not appear to have SSDA in our datasets, however, a Hsp90 ATPase was observed in similar patterns to Hsp70 in the A15-ARP23 to A15 and A15-ARP23 to ARP23 comparison with an additional finding

of reduced abundance in the A15-CWH to CWH comparison. This cochaperone of the Hsp90 system stimulates the ATPase activity of Hsp90 and loss of function results in heightened sensitivity to conditions of elevated stress (Panaretou et al., 2002). Further evidence of a stress-response was provided via heightened abundances of hydrophobins in the A15-ARP23 interaction (**Figure 5**). Hydrophobins are implicated in stress-response due to their importance in the production of aerial hyphae growth, as they confer hydrophobicity to aerial hyphae and prevent collapse through the weight of ambient moistures etc. (Mikus et al., 2009; Mosbach et al., 2011). The heightened levels of hydrophobins may play a role in the uncharacteristic fluffy growths observed in the A15-ARP23 co-culture, although it should be noted that hydrophobin levels in A15-A15 co-cultures were also high, albeit, not to the same degree as the A15-ARP23 co-culture (**Figure 5**). The heterokaryon incompatibility system (*het*) was also induced during the interaction of A15 and ARP23. Het-C plays a role in the recognition of self and non-self (Wu et al., 1998). This finding suggests that A15 and ARP23 are sufficiently divergent to trigger a system designed to maintain colony individuality. Furthermore, three putative laccases were found as SSDA only in the A15-ARP23 co-culture (**Table_S5)**. This may be an indicator that these enzymes play an important role in the antagonism observed between the two strains. Laccases have been found to increase in terms of their abundance and activity during interspecific interactions in white-rot fungi (Baldrian, 2004; Freitag and Morrel, 1992; Zhong et al., 2018) and are implicated with oxidation of xenobiotic compounds and general detoxification (Kües, 2007). Laccase is involved in the melanin synthesis (Nagai, 2003). Cell wall integrity is heightened by melanin (Brush and Money, 1999). ARP23 is a wild isolate strain with a brown fruiting body phenotype and highly melanised hyphae relative to other commercial cultivar mycelium. High levels of laccases in ARP23 co-culture may point to an endurance strategy adopted by this strain by strengthening its hyphae during antagonistic interactions.

As A15 and CWH do not readily anastomose (**Figure 2B**), it is possible that they do not readily 'fuse into a single colony' *in vitro* as seen for other vegetative-compatible dual-culture interactions (**Figure 2A&C**). Evidence of nitrogen starvation mechanisms may provide further evidence for this observation, as nitrogen metabolism may be subverted to internal urea as a new nitrogen source. Moreover, many SSDA proteins found to be highly abundant in the A15-A15 and A15-ARP23 co-cultures were either absent in the A15-CWH co-culture or in significantly lower abundances (**Table_S2**). A possible reason for this may be that both strains are effective at not interacting with one another. In terms of anastomosis, A15-CWH and A15-ARP23 interactions are not dissimilar, however, the A15-ARP23 interaction goes beyond lack of anastomosis and into antagonism as reflected in their proteomic profiles (**Figure** 5) and phenotypic evidence of uncharacteristic fluffiness of hyphal growth (**Figure 2B**).

Our proteomic analyses illustrate the differences between vegetative compatibility and incompatibility (**Figure 4)**. Fundamental housekeeping processes and substrate metabolism are all highest when A15 is paired with itself. By comparing co-culture SSDA protein sets, a number of proteins were captured as common to all interactions (not at strain-level) and unique to certain interactions (strain-level). In summary, proteomic responses of hypha-hypha interactions between the three strains of *A. bisporus* were investigated using an *in vitro* co-culture interaction design and a label-free/nontargeted approach of proteomic profiling. Even at the strain-level, a variety of changes were observed in interacting cultures ranging from proteins pertinent to hyphal morphology, carbohydrate metabolism, stress responses, *het* system-related proteins and nitrogen metabolism.

5. Conclusion

This is the first study to characterise the proteomic response of three interacting *A. bisporus* strains ranging from full vegetative compatibility to incompatibility. New insights into pathways and candidate proteins vital to anastomosis have been discussed. Our analyses shows that vegetative compatible interactions are represented by high levels of carbohydrate metabolism in the form of cell wall biogenesis, modification, and expansion. With respect to co-cultures, A15-CWH represents less of an antagonistic interaction and more of a competitive interaction for substrate, reflected by high levels of oxidoreductase activity and nitrogen-starvation responses. In terms of hyphal interaction, comparative protein abundances relative to the other interactions suggest A15 and CWH are likely interacting much less. Conversely, the A15-ARP23 interaction is most highly representative of a vegetative incompatibility and antagonism, represented by high levels of LDA enzymes and hydrophobins. This study has provided insight into the how the proteomic response of different strains of *A. bisporus* can lead to vegetative incompatible interactions and therefore, reinforce the use of these strains as disease-breakers in commercial mushroom crops. Additionally, new insights have been gained into the proteomic response of a range of vegetative compatibilities during inter-hyphal interactions of this filamentous fungus that may guide future studies relating to anastomosis.

682

683 **Acknowledgments**

684 EOC is funded by a Teagasc Walsh Fellowship Scheme (grant reference number 10564231).
685 We acknowledge the DJEI/DES/SFI/HEA Irish Centre for High-End Computing (ICHEC)
686 for the provision of computational facilities and support. Mass spectrometry facilities were
687 funded by Science Foundation Ireland (SFI 12/RI/2346(3)).

688

689 **Figure legends**

690 **Figure 1:** Representation of the demarcation zone between two neighbouring vegetative-
691 compatible strains of *A. bisporus* mycelia originating from opposite directions. The substrate
692 area is covered by the apical extension of a main/leading hypha which continuously generates
693 primary branches which may be subtended by secondary branches. Anastomoses are most
694 frequently observed in branching hyphae but may occasionally be seen in leading hyphae.
695 Orange arrows represent self-anastomoses and blue arrows represent non-self anastomoses.

696 **Figure 2:** Interactions between different strains of *A. bisporus* grown on cellophane
697 membranes on CYM. **A**: A15 paired with A15; Note areas where hyphae cross culture
698 boundaries primarily at the top and bottom of the interaction zones. **B**: A15 (left colony)
699 paired with CWH (right colony); Cultures appear to repel one another, with no visible hyphal
700 crossover. **C**: A15 (left colony) interacting with ARP23 (right colony); A highly defined zone
701 of interaction is clear. Formation of 'fluffy' growth in plumes of hyphae can be seen at the
702 top and bottom of A15 and in the three panels from other A15-ARP23 replicate plates.

703 **Figure 3**: SSDA proteins from the whole proteome of each monoculture and co-culture. Non-
704 axial horizontal lines represent $-\log_{10} P$ cut-off ($P < 0.05$ prior to transformation) and non-

axial vertical lines represent log_2 fold change (FC) ±1.5. Data points which are coloured in the top left quadrant are significantly increased in abundance in monocultures and data points coloured in the top right quadrant are significantly increased in abundance in co-cultures.

Figure 4: KEGG analysis of whole proteomes from each monoculture and co-culture. Functional annotation of each proteome was made through aligning protein sequences to known KEGG genes and categories were formed based on high-level functionality.

Figure 5: Secreted and extracellular SSDA proteins of comparisons of monoculture to co-culture interactions that potentially play important roles in anastomosis. Accession numbers (AC) of each protein is provided. And are preceded by the Joint Genome Institute (JGI) identifier 'jgi|Agabi_varbisH97_2'. Fold change ranges are of log_2 transformed LFQ intensities. Grey tiles indicate proteins which did not fall within SSDA criteria or may not have been detected.

Figure 6: Selected CAZymes from monoculture and strain A15 co-cultures. **A**: Comparisons of the number of proteins found in each CAZyme class in monocultures and co-cultures. **B**: Shared and unique CAZymes in A15-CWH co-culture and respective monocultures. **C**: Shared and unique CAZymes in A15-ARP23 co-culture and respective monocultures.

Figure 7: Differentially abundant proteins (SSDA) detected in comparisons between co-cultures (A15-A15, A15-CWH, A15-ARP23) and the A15 monoculture.

728

729

730

731

732

733

734 **Literature Cited**

735 Ahmad, I., Hellebust, J.A., 1991. 7 Enzymology of Nitrogen Assimilation in Mycorrhiza, in:
736 Methods in Microbiology. pp. 181–202.

737 Ainsworth, A.M., Rayner, A.D.M., 1986. Responses of Living Hyphae Associated with Self
738 and Non-self Fusions in the Basidiomycete *Phanerochaete velutina*. Microbiology 132,
739 pp. 191–201.

740 Ashburner, M., Ball, C.A., Blake, J.A., Botstein, D., Butler, H., Cherry, J.M., Davis, A.P.,
741 Dolinski, K., Dwight, S.S., Eppig, J.T., Harris, M.A., Hill, D.P., Issel-Tarver, L.,
742 Kasarskis, A., Lewis, S., Matese, J.C., Richardson, J.E., Ringwald, M., Rubin, G.M.,
743 Sherlock, G., 2000. Gene Ontology: tool for the unification of biology. Nat. Genet. 25,
744 pp. 25–29.

745 Baars, J.J.P., Op den Camp, H.J.M., Hermans, J.M.H., Mikes, V., van der Drift, C., Van
746 Griensven, L.J.L.D., Vogels, G.D., 1994. Nitrogen assimilating enzymes in the white
747 button mushroom *Agaricus bisporus*. Microbiology 140, pp. 1161–1168.

748 Babich, M., Foti, L.R.P., Sykaluk, L.L., Clark, C.R., 1996. Profilin Forms Tetramers That
749 Bind to G-Actin. Biochem. Biophys. Res. Commun. 218, pp. 125–131.

750 Bakker, B., 2001. Stoichiometry and compartmentation of NADH metabolism in
751 *Saccharomyces cerevisiae*. FEMS Microbiol. Rev. 25, pp. 15–37.

752 Balakrishnan, R., Park, J., Karra, K., Hitz, B.C., Binkley, G., Hong, E.L., Sullivan, J.,
753 Micklem, G., Michael Cherry, J., 2012. YeastMine—an integrated data warehouse for
754 *Saccharomyces cerevisiae* data as a multipurpose tool-kit. Database 2012.

755 Baldrian, P., 2004. Increase of laccase activity during interspecific interactions of white-rot
756 fungi. FEMS Microbiol. Ecol. 50, pp. 245–253.

757 Bartnicki-Garcia, S., Hergert, F., Gierz, G., 1989. Computer simulation of fungal
758 morphogenesis and the mathematical basis for hyphal (tip) growth. Protoplasma 153, pp.
759 46–57.

760 Beckers, G., Bendt, A.K., Kramer, R., Burkovski, A., 2004. Molecular Identification of the
761 Urea Uptake System and Transcriptional Analysis of Urea Transporter- and Urease-
762 Encoding Genes in *Corynebacterium glutamicum*. J. Bacteriol. 186, pp. 7645–7652.

763 Beites, T., Oliveira, P., Rioseras, B., Pires, S.D.S., Oliveira, R., Tamagnini, P., Moradas-
764 Ferreira, P., Manteca, Á., Mendes, M. V., 2015. *Streptomyces natalensis* programmed
765 cell death and morphological differentiation are dependent on oxidative stress. Sci. Rep.
766 5, 12887.

767 Bendtsen, J.D., Jensen, L.J., Blom, N., von Heijne, G., Brunak, S., 2004. Feature-based
768 prediction of non-classical and leaderless protein secretion. Protein Eng. Des. Sel. 17,
769 pp. 349–356.

770 Biella, S., Smith, M.L., Aist, J.R., Cortesi, P., Milgroom, M.G., 2002. Programmed cell death
771 correlates with virus transmission in a filamentous fungus. Proc. R. Soc. London. Ser. B
772 Biol. Sci. 269, pp. 2269–2276.

773 Boddy, L., 2000. Interspecific combative interactions between wood-decaying
774 basidiomycetes. FEMS Microbiol. Ecol. 31, pp. 185–194.

775 Bourges, N., Groppi, A., Barreau, C., Clavé, C., Bégueret, J., 1998. Regulation of gene
776 expression during the vegetative incompatibility reaction in Podospora anserina.
777 Characterization of three induced genes. Genetics 150, pp. 633–41.

778 Brush, L., Money, N.P., 1999. Invasive Hyphal Growth in *Wangiella dermatitidis* Is Induced
779 by Stab Inoculation and Shows Dependence upon Melanin Biosynthesis. Fungal Genet.

780 Biol. 28, pp. 190–200.

781 Cabib, E., 2009. Two Novel Techniques for Determination of Polysaccharide Cross-Links
782 Show that Crh1p and Crh2p Attach Chitin to both β(1-6)- and β(1-3)Glucan in the
783 *Saccharomyces cerevisiae* Cell Wall. Eukaryot. Cell 8, 1626–1636.

784 Callac, P., Imbernon, M., Kerrigan, R.W., Olivier, J.-M., 1996. A summary of allelic
785 diversity and geographical distribution at six allozyme loci of *Agaricus bisporus*.
786 Mushroom Biol. Mushroom Prod. pp. 57–66.

787 Cantarel, B.L., Coutinho, P.M., Rancurel, C., Bernard, T., Lombard, V., Henrissat, B., 2009.
788 The Carbohydrate-Active EnZymes database (CAZy): an expert resource for
789 Glycogenomics. Nucleic Acids Res. 37, D233–D238.

790 Chu, Y.-M., Jeon, J.-J., Yea, S.-J., Kim, Y.-H., Yun, S.-H., Lee, Y.-W., Kim, K.-H., 2002.
791 Double-Stranded RNA Mycovirus from *Fusarium graminearum*. Appl. Environ.
792 Microbiol. 68, pp. 2529–2534.

793 Claydon, N., Allan, M., Wood, D.A., 1988. Fruit body biomass regulated production of
794 extracellular endocellulase during periodic fruiting by *Agaricus bisporus*. Trans. Br.
795 Mycol. Soc. 90, pp. 85–90.

796 Collins, C., Keane, T.M., Turner, D.J., O'Keeffe, G., Fitzpatrick, D.A., Doyle, S., 2013.
797 Genomic and Proteomic Dissection of the Ubiquitous Plant Pathogen, *Armillaria*
798 *mellea* : Toward a New Infection Model System. J. Proteome Res. 12, pp. 2552–2570.

799 Cox, J., Mann, M., 2008. MaxQuant enables high peptide identification rates, individualized
800 p.p.b.-range mass accuracies and proteome-wide protein quantification. Nat. Biotechnol.
801 26, pp. 1367–1372.

802 Davis, L.L., Bartnicki-Garcia, S., 1984. Chitosan synthesis by the tandem action of chitin

synthetase and chitin deacetylase from *Mucor rouxii*. Biochemistry 23, pp. 1065–1073.

Dyrløv Bendtsen, J., Nielsen, H., von Heijne, G., Brunak, S., 2004. Improved Prediction of Signal Peptides: SignalP 3.0. J. Mol. Biol. 340, pp. 783–795.

El Ariebi, N., Hiscox, J., Scriven, S.A., Müller, C.T., Boddy, L., 2016. Production and effects of volatile organic compounds during interspecific interactions. Fungal Ecol. 20, pp. 144–154.

Fermor, T.R., Wood, D.A., Lincoln, S.P., Fenlon, J.S., 1991. Bacteriolysis by *Agaricus bisporus*. J. Gen. Microbiol. 137, pp. 15–22.

Ferreira, P., Carro, J., Serrano, A., Martinez, A.T., 2015. A survey of genes encoding H2O2-producing GMC oxidoreductases in 10 Polyporales genomes. Mycologia 107, pp. 1105–1119.

Flärdh, K., Buttner, M.J., 2009. Streptomyces morphogenetics: dissecting differentiation in a filamentous bacterium. Nat. Rev. Microbiol. 7, pp. 36–49.

Fletcher, J., H. Gaze, R., 2007. Mushroom Pest and Disease Control, Mycological Research. CRC Press.

Freitag, M., Morrel, J.J., 1992. Changes in selected enzyme activities during growth of pure and mixed cultures of the white-rot decay fungus *Trametes versicolor* and the potential biocontrol fungus *Trichoderma harzianum*. Can. J. Microbiol. 38, pp. 317–323.

Garnjobst, L., Wilson, J.F., 1956. Heterocaryosis and protoplasmic incompatibility in *Neurospora crassa*. Proc. Natl. Acad. Sci. 42, pp. 613–618.

Girbardt, M., 1969. Die Ultrastruktur der Apikalregion von Pilzhyphen. Protoplasma 67, pp. 413–441.

825 Girbardt, M., 1957. Der Spitzenkörper von *Polystictus versicolor* (L.). Planta 50, 47–59.

826 Glass, N., 2004. Hyphal homing, fusion and mycelial interconnectedness. Trends Microbiol.
827 12, pp. 135–141.

828 Glass, N.L., Fleissner, A., 2006. Re-Wiring the Network: Understanding the Mechanism and
829 Function of Anastomosis in Filamentous Ascomycete Fungi, in: Growth, Differentiation
830 and Sexuality. Springer-Verlag, Berlin/Heidelberg, pp. 123–139.

831 Glass, N.L., Jacobson, D.J., Shiu, P.K.T., 2000. The Genetics of Hyphal Fusion and
832 Vegetative Incompatibility in Filamentous Ascomycete Fungi. Annu. Rev. Genet. 34,
833 pp. 165–186.

834 Glass, N.L., Kuldau, G.A., 1992. Mating Type and Vegetative Incompatibility in Filamentous
835 Ascomycetes. Annu. Rev. Phytopathol. 30, pp. 201–224.

836 Grogan, H.M., Adie, B.A.T., Gaze, R.H., Challen, M.P., Mills, P.R., 2003. Double-stranded
837 RNA elements associated with the MVX disease of *Agaricus bisporus*. Mycol. Res. 107,
838 pp. 147–154.

839 Grogan, H.M., Tomprefa, N., J., M., Holcroft, S., Gaze, R., 2004. Transmission of Mushroom
840 Virus X Disease in crops. Mushroom Sci. 16, pp. 489–498.

841 Guillamon, J., Vanriel, N., Giuseppin, M., Verrips, C., 2001. The glutamate synthase
842 (GOGAT) of plays an important role in central nitrogen metabolism. FEMS Yeast Res.
843 1, pp. 169–175.

844 Hansberg, W., Aguirre, J., 1990. Hyperoxidant states cause microbial cell differentiation by
845 cell isolation from dioxygen. J. Theor. Biol. 142, pp. 201–221.

846 Harris, S., 2001. Septum formation in Aspergillus nidulans. Curr. Opin. Microbiol. 4, pp.
847 736–739.

Hartland, R.P., Fontaine, T., Debeaupuis, J.-P., Simenel, C., Delepierre, M., Latgé, J.-P., 1996. A Novel β-(1, 3,)-Glucanosyltransferase from the Cell Wall of *Aspergillus fumigatus*. J. Biol. Chem. 271, pp. 26843–26849.

Herrmann, K.M., Weaver, L.M., 1999. The shikimate pathway. Annu. Rev. Plant Physiol. Plant Mol. Biol. 50, pp. 473–503.

Hiscox, J., Savoury, M., Toledo, S., Kingscott-Edmunds, J., Bettridge, A., Waili, N. Al, Boddy, L., 2017. Threesomes destabilise certain relationships: multispecies interactions between wood decay fungi in natural resources. FEMS Microbiol. Ecol. 93.

Jones, P., Binns, D., Chang, H.-Y., Fraser, M., Li, W., McAnulla, C., McWilliam, H., Maslen, J., Mitchell, A., Nuka, G., Pesseat, S., Quinn, A.F., Sangrador-Vegas, A., Scheremetjew, M., Yong, S.-Y., Lopez, R., Hunter, S., 2014. InterProScan 5: genome-scale protein function classification. Bioinformatics 30, pp. 1236–40.

Kabel, M.A., Jurak, E., Mäkelä, M.R., de Vries, R.P., 2017. Occurrence and function of enzymes for lignocellulose degradation in commercial *Agaricus bisporus* cultivation. Appl. Microbiol. Biotechnol. 101, pp. 4363–4369.

Kall, L., Krogh, A., Sonnhammer, E.L.L., 2007. Advantages of combined transmembrane topology and signal peptide prediction--the Phobius web server. Nucleic Acids Res. 35, W429–W432.

Kanehisa, M., Sato, Y., Morishima, K., 2016. BlastKOALA and GhostKOALA: KEGG Tools for Functional Characterization of Genome and Metagenome Sequences. J. Mol. Biol. 428, pp.726–731.

Kashif, M., Jurvansuu, J., Vainio, E.J., Hantula, J., 2019. Alphapartitiviruses of Heterobasidion Wood Decay Fungi Affect Each Other's Transmission and Host Growth.

Front. Cell. Infect. Microbiol. 9, 64.

Khan, A., McQuilken, M., Gladfelter, A.S., 2015. Septins and Generation of Asymmetries in Fungal Cells. Annu. Rev. Microbiol. 69, pp. 487–503.

Knoll, A.H., 2011. The Multiple Origins of Complex Multicellularity. Annu. Rev. Earth Planet. Sci. 39, pp. 217–239.

Kovar, D.R., Harris, E.S., Mahaffy, R., Higgs, H.N., Pollard, T.D., 2006. Control of the Assembly of ATP- and ADP-Actin by Formins and Profilin. Cell 124, pp. 423–435.

Kües, U. (Ed.), 2007. Wood production, wood technology, and biotechnological impacts, Wood production, wood technology, and biotechnological impacts. Göttingen University Press, Göttingen 635 p.

Labarere, J., Bernet, J., 1977. Protoplasmic Incompatibility and Cell Lysis in *Podospora anserina*. I. Genetic Investigations on Mutations of a Novel Modifier Gene That Suppresses Cell Destruction. Genetics 87, pp. 249–57.

Leslie, J.F., 1993. Fungal Vegetative Compatibility. Annu. Rev. Phytopathol. 31, 127–150.

Lipke, P., 2018. What We Do Not Know about Fungal Cell Adhesion Molecules. J. Fungi 4, 59.

Löpez-Franco, R., Bracker, C.E., 1996. Diversity and dynamics of the Spitzenkörper in growing hyphal tips of higher fungi. Protoplasma 195, pp. 90–111.

Manning, K., Wood, D.A., 1984. Cellulase production and regulation by *Agaricus bisporus*. Appl. Biochem. Biotechnol. 9, pp. 385–386.

Markham, P., 1994. Occlusions of septal pores in filamentous fungi. Mycol. Res. 98, pp. 1089–1106.

Mikus, M., Hatvani, L., Neuhof, T., Komon-Zelazowska, M., Dieckmann, R., Schwecke, T., Druzhinina, I.S., von Dohren, H., Kubicek, C.P., 2009. Differential Regulation and Posttranslational Processing of the Class II Hydrophobin Genes from the Biocontrol Fungus *Hypocrea atroviridis*. Appl. Environ. Microbiol. 75, pp. 3222–3229.

Mobley, H.L., Hausinger, R.P., 1989. Microbial ureases: significance, regulation, and molecular characterization. Microbiol. Rev. 53, pp. 85–108.

Mogk, A., Deuerling, E., Vorderwülbecke, S., Vierling, E., Bukau, B., 2003. Small heat shock proteins, ClpB and the DnaK system form a functional triade in reversing protein aggregation. Mol. Microbiol. 50, pp. 585–595.

Morin, E., Kohler, A., Baker, A.R., Foulongne-Oriol, M., Lombard, V., Nagye, L.G., Ohm, R. a., Patyshakuliyeva, A., Brun, A., Aerts, A.L., Bailey, A.M., Billette, C., Coutinho, P.M., Deakin, G., Doddapaneni, H., Floudas, D., Grimwood, J., Hilden, K., Kues, U., LaButti, K.M., Lapidus, A., Lindquist, E.A., Lucas, S.M., Murat, C., Riley, R.W., Salamov, A. a., Schmutz, J., Subramanian, V., Wosten, H. a. B., Xu, J., Eastwood, D.C., Foster, G.D., Sonnenberg, A.S.M., Cullen, D., de Vries, R.P., Lundell, T., Hibbett, D.S., Henrissat, B., Burton, K.S., Kerrigan, R.W., Challen, M.P., Grigoriev, I. V., Martin, F., 2012. Genome sequence of the button mushroom *Agaricus bisporus* reveals mechanisms governing adaptation to a humic-rich ecological niche. Proc. Natl. Acad. Sci. 109, pp. 17501–17506.

Mosbach, A., Leroch, M., Mendgen, K.W., Hahn, M., 2011. Lack of evidence for a role of hydrophobins in conferring surface hydrophobicity to conidia and hyphae of *Botrytis cinerea*. BMC Microbiol. 11, 10.

Nagai, M., 2003. Important role of fungal intracellular laccase for melanin synthesis: purification and characterization of an intracellular laccase from *Lentinula edodes* fruit

bodies. Microbiology 149, pp. 2455–2462.

Nagy, L.G., Kovács, G.M., Krizsán, K., 2018. Complex multicellularity in fungi: evolutionary convergence, single origin, or both? Biol. Rev. 93, 1778–1794.

Nelson, R.J., Ziegelhoffer, T., Nicolet, C., Werner-Washburne, M., Craig, E.A., 1992. The translation machinery and 70 kd heat shock protein cooperate in protein synthesis. Cell 71, pp. 97–105.

O'Connor, E., McGowan, J., McCarthy, C.G.P., Amini, A., Grogan, H., Fitzpatrick, D.A., 2019. Whole Genome Sequence of the Commercially Relevant Mushroom Strain *Agaricus bisporus* var. bisporus ARP23. G3 (Bethesda). g3.400563.2019.

O'Keeffe, G., Hammel, S., Owens, R.A., Keane, T.M., Fitzpatrick, D.A., Jones, G.W., Doyle, S., 2014. RNA-seq reveals the pan-transcriptomic impact of attenuating the gliotoxin self-protection mechanism in *Aspergillus fumigatus*. BMC Genomics 15, 894.

Ogata, H., Goto, S., Sato, K., Fujibuchi, W., Bono, H., Kanehisa, M., 1999. KEGG: Kyoto Encyclopedia of Genes and Genomes. Nucleic Acids Res. 27, pp. 29–34.

Owens, R.A., O'Keeffe, G., Smith, E.B., Dolan, S.K., Hammel, S., Sheridan, K.J., Fitzpatrick, D.A., Keane, T.M., Jones, G.W., Doyle, S., 2015. Interplay between Gliotoxin Resistance, Secretion, and the Methyl/Methionine Cycle in *Aspergillus fumigatus*. Eukaryot. Cell 14, pp. 941–957.

Panaretou, B., Siligardi, G., Meyer, P., Maloney, A., Sullivan, J.K., Singh, S., Millson, S.H., Clarke, P.A., Naaby-Hansen, S., Stein, R., Cramer, R., Mollapour, M., Workman, P., Piper, P.W., Pearl, L.H., Prodromou, C., 2002. Activation of the ATPase Activity of Hsp90 by the Stress-Regulated Cochaperone Aha1. Mol. Cell 10, pp. 1307–1318.

940 Paoletti, M., Clavé, C., 2007. The Fungus-Specific HET Domain Mediates Programmed Cell
941 Death in *Podospora anserina*. Eukaryot. Cell 6, pp. 2001–2008.

942 Pontecorvo, G., 1956. The Parasexual Cycle in Fungi. Annu. Rev. Microbiol. 10, pp. 393–
943 400.

944 Pontecorvo, G., Roper, J.A., Forbes, E., 1953. Genetic Recombination without Sexual
945 Reproduction in *Aspergillus niger*. J. Gen. Microbiol. 8, pp. 198–210.

946 Pontes, M.V.A., Patyshakuliyeva, A., Post, H., Jurak, E., Hildén, K., Altelaar, M., Heck, A.,
947 Kabel, M.A., de Vries, R.P., Mäkelä, M.R., 2018. The physiology of *Agaricus bisporus*
948 in semi-commercial compost cultivation appears to be highly conserved among
949 unrelated isolates. Fungal Genet. Biol. 112, pp. 12–20.

950 Ragni, E., Fontaine, T., Gissi, C., Latgè, J.P., Popolo, L., 2007. The Gas family of proteins of
951 *Saccharomyces cerevisiae*: characterization and evolutionary analysis. Yeast 24, 297–
952 308.

953 Rangamani, P., Xiong, G.Y., Iyengar, R., 2014. Multiscale modeling of cell shape from the
954 actin cytoskeleton. Prog. Mol. Biol. Transl. Sci. 123, pp. 143–67.

955 Raychaudhuri, S., Prinz, W.A., 2010. The Diverse Functions of Oxysterol-Binding Proteins.
956 Annu. Rev. Cell Dev. Biol. 26, pp. 157–177.

957 Reynaga-Pena, C.G., Gierz, G., Bartnicki-Garcia, S., 1997. Analysis of the role of the
958 Spitzenkorper in fungal morphogenesis by computer simulation of apical branching in
959 *Aspergillus niger*. Proc. Natl. Acad. Sci. 94, pp. 9096–9101.

960 Riquelme, M., Bartnicki-Garcia, S., 2004. Key differences between lateral and apical
961 branching in hyphae of *Neurospora crassa*. Fungal Genet. Biol. 41, pp. 842–851.

962 Riquelme, M., Roberson, R.W., Sánchez-León, E., 2016. 3 Hyphal Tip Growth in

963 Filamentous Fungi, in: Growth, Differentiation and Sexuality. Springer International
964 Publishing, Cham, pp. 47–66.

965 Romaine, C.P., Ulhrich, P., Schlagnhaufer, B., 1993. Transmission of La France Isometric
966 Virus during Basidiosporogenesis in *Agaricus bisporus*. Mycologia 85, 175.

967 Saporito-Irwin, S.M., Birse, C.E., Sypherd, P.S., Fonzi, W.A., 1995. PHR1, a pH-regulated
968 gene of *Candida albicans*, is required for morphogenesis. Mol. Cell. Biol. 15, pp. 601–
969 613.

970 Sarkar, S., 2002. Nonself recognition is mediated by HET-C heterocomplex formation during
971 vegetative incompatibility. EMBO J. 21, pp. 4841–4850.

972 Schöneberg, A., Musa, T., Voegele, R.T., Vogelgsang, S., 2015. The potential of antagonistic
973 fungi for control of Fusarium graminearum and *Fusarium crookwellense* varies
974 depending on the experimental approach. J. Appl. Microbiol. 118, pp. 1165–1179.

975 Silar, P., 2005. Peroxide accumulation and cell death in filamentous fungi induced by contact
976 with a contestant. Mycol. Res. 109, pp. 137–149.

977 Sipos, G., Prasanna, A.N., Walter, M.C., O'Connor, E., Bálint, B., Krizsán, K., Kiss, B.,
978 Hess, J., Varga, T., Slot, J., Riley, R., Bóka, B., Rigling, D., Barry, K., Lee, J.,
979 Mihaltcheva, S., LaButti, K., Lipzen, A., Waldron, R., Moloney, N.M., Sperisen, C.,
980 Kredics, L., Vágvölgyi, C., Patrignani, A., Fitzpatrick, D., Nagy, I., Doyle, S.,
981 Anderson, J.B., Grigoriev, I. V., Güldener, U., Münsterkötter, M., Nagy, L.G., 2017.
982 Genome expansion and lineage-specific genetic innovations in the forest pathogenic
983 fungi Armillaria. Nat. Ecol. Evol. 1, pp. 1931–1941.

984 Smith, M.L., Gibbs, C.C., Milgroom, M.G., 2006. Heterokaryon incompatibility function of
985 barrage-associated vegetative incompatibility genes (vic) in *Cryphonectria parasitica*.

Mycologia 98, pp. 43–50.

Sonnenberg, A.S.M., Baars, J.J.P., Gao, W., Visser, R.G.F., 2017. Developments in breeding of *Agaricus bisporus* var. *bisporus*: progress made and technical and legal hurdles to take. Appl. Microbiol. Biotechnol. 101, 1819–1829.

Sonnhammer, E.L., von Heijne, G., Krogh, A., 1998. A hidden Markov model for predicting transmembrane helices in protein sequences. Proceedings. Int. Conf. Intell. Syst. Mol. Biol. 6, pp. 175–82.

Sperschneider, J., Williams, A.H., Hane, J.K., Singh, K.B., Taylor, J.M., 2015. Evaluation of Secretion Prediction Highlights Differing Approaches Needed for Oomycete and Fungal Effectors. Front. Plant Sci. 6, 1168.

Swart, K., Debets, a J., Bos, C.J., Slakhorst, M., Holub, E.F., Hoekstra, R.F., 2001. Genetic analysis in the asexual fungus *Aspergillus niger*. Acta Biol. Hung. 52, pp. 335–43.

Takaya, N., Yamazaki, D., Horiuchi, H., Ohta, A., Takagi, M., 1998. Intracellular chitinase gene from *Rhizopus oligosporus*: molecular cloning and characterization. Microbiology 144, pp. 2647–2654.

Takaya, N., Yamazaki, D., Horiuchi, H., Ohta, A., Takagi, M., 1998. Cloning and Characterization of a Chitinase-encoding Gene (chiA) from *Aspergillus nidulans* , Disruption of Which Decreases Germination Frequency and Hyphal Growth. Biosci. Biotechnol. Biochem. 62, pp. 60–65.

Tiwari, S., Thakur, R., Shankar, J., 2015. Role of Heat-Shock Proteins in Cellular Function and in the Biology of Fungi. Biotechnol. Res. Int. 2015, pp. 1–11.

Tsigos, I., Bouriotis, V., 1995. Purification and Characterization of Chitin Deacetylase from Colletotrichum lindemuthianum. J. Biol. Chem. 270, pp. 26286–26291.

1009 Tyanova, S., Temu, T., Sinitcyn, P., Carlson, A., Hein, M.Y., Geiger, T., Mann, M., Cox, J.,
1010 2016. The Perseus computational platform for comprehensive analysis of (prote)omics
1011 data. Nat. Methods 13, pp. 731–740.

1012 Van Bael, S.A., Fernández-Marín, H., Valencia, M.C., Rojas, E.I., Wcislo, W.T., Herre, E.A.,
1013 2009. Two fungal symbioses collide: endophytic fungi are not welcome in leaf-cutting
1014 ant gardens. Proc. R. Soc. B Biol. Sci. 276, pp. 2419–2426.

1015 van Diepeningen, A.D., Debets, A.J.M., Hoekstra, R.F., 1998. Intra- and Interspecies Virus
1016 Transfer in Aspergilli via Protoplast Fusion. Fungal Genet. Biol. 25, pp. 171–180.

1017 Van Griensven, L.J.L.D., 1987. The Cultivation of Mushrooms: Its Present Status and Future
1018 Developments. Outlook Agric. 16, pp. 131–135.

1019 Van Zaayen, A., 1978. Resistance of *Agaricus* species other than *bisporus* to mushroom virus
1020 disease. Mushroom Science X, Proceedings of the 10th international Congress on the science
1021 and cultivation of Edible Fungi, France, 1978. Part 1: 759-772

1022

1023 Vedder, P.J.C., 1978. Modern mushroom growing. Educaboek.

1024 Wagemaker, M.J.M., Eastwood, D.C., van der Drift, C., Jetten, M.S.M., Burton, K., Van
1025 Griensven, L.J.L.D., Op den Camp, H.J.M., 2006. Expression of the urease gene of
1026 Agaricus bisporus: a tool for studying fruit body formation and post-harvest
1027 development. Appl. Microbiol. Biotechnol. 71, pp. 486–492.

1028 Wood, D.A., Thurston, C.F., 1991. Progress in the molecular analysis of Agaricus enzymes.
1029 Genet. Breed. Agaricus. Proc. First Int. Semin. Mushroom Sci. Mushroom Exp. Station.
1030 Horst, Netherlands, 14-17 May 1991. pp. 81–86.

1031 Wu, J., Saupe, S.J., Glass, N.L., 1998. Evidence for balancing selection operating at the het-c

heterokaryon incompatibility locus in a group of filamentous fungi. Proc. Natl. Acad. Sci. 95, pp. 12398–12403.

Yague, E., Mehak-Zunic, M., Morgan, L., Wood, D.A., Thurston, C.F., 1997. Expression of CEL2 and CEL4, Two Proteins from *Agaricus bisporus* with Similarity to Fungal Cellobiohydrolase I and -mannanase, Respectively, is Regulated by the Carbon Source. Microbiology 143, pp. 239–244.

Zhang, H., Yohe, T., Huang, L., Entwistle, S., Wu, P., Yang, Z., Busk, P.K., Xu, Y., Yin, Y., 2018. dbCAN2: a meta server for automated carbohydrate-active enzyme annotation. Nucleic Acids Res. 46, W95–W101.

Zhong, Z., Li, N., Liu, L., He, B., Igarashi, Y., Luo, F., 2018. Label-free differentially proteomic analysis of interspecific interaction between white-rot fungi highlights oxidative stress response and high metabolic activity. Fungal Biol. 122, pp. 774–784.

Table 1: Proteins found exclusively in ARP23 monoculture and co-culture. Proteins were unambiguously mapped to the genome of *A. bisporus var. bisporus* (ARP23) only, with none mapping to *A. bisporus var. bisporus* (H97) after peptide scoring of the ARP23 and H97 concatenated database. Proteins found exclusively in sample replicates (*n* =2/3) of ARP23 or A15-ARP23 were considered.

	Accession No.[a]	Pfams	Description[b]	GO Description	Unique peptides	Sequence coverage [%]	Mol. weight [kDa]
ARP23 - Monoculture	**08516**	PF01263	Aldose 1-epimerase	GO:0016853: Isomerase activity; GO:0005975: Carbohydrate metabolic process	2	59.3	42.13
	09378	No Pfam	-	No GO Terms	9	50.2	22.288
	00967	PF00561	Alpha/beta hydrolase fold	No GO Terms	2	63.7	35.265
	01587	PF13561	Enoyl-reductase	No GO Terms	3	27.6	27.077
	02545	PF07249	Cerato-platanin	No GO Terms	2	47.4	16.514
	03883	PF00734, PF01341	GH6	GO:0030248: Cellulose binding; GO:0005975: Carbohydrate metabolic process; GO:0030245: Cellulose catabolic process; GO:0005576: Extracellular region; GO:0004553: Hydrolase	4	75.6	46.168

			activity, hydrolyzing O-glycosyl compounds			
05644	No Pfam	na	No GO Terms	1	46.7	31.729
07238	PF01915, PF00933	GH3	GO:0004553: Hydrolase activity, hydrolyzing O-glycosyl compounds; GO:0005975: Carbohydrate metabolic process	1	58.1	95.432
07366	PF00108, PF02803	Thiolase	GO:0016747: Transferase activity, transferring acyl groups other than amino-acyl groups	1	56.9	28.53
10146	PF13363, PF10435, PF13364, PF01301	Beta-galactosidase/GH35	No GO Terms	3	44.5	106.14
10232	No Pfam		No GO Terms	6	35.1	39.876
11520	PF01764	Lipase	GO:0006629: Lipid metabolic process	1	35.6	31.11
12240	PF01423	LSM domain	No GO Terms	3	18.7	17.898

01577	PF00795	Carbon-nitrogen hydrolase	GO:0006807: Nitrogen compound metabolic process	2	54.1	35.293
02924	PF00208	Glutamate/Leucine/Phenylalanine/Valine dehydrogenase	GO:0016491: Oxidoreductase activity; GO:0006520: Cellular amino acid metabolic process; GO:0055114: Oxidation-reduction process	1	63.9	29.122
05228	PF00012	Hsp70 protein	No GO Terms	4	55.6	73.502
09093	PF00012	Hsp70 protein	No GO Terms	2	64.5	88.11
09149	PF03556, PF14555	Cullin binding	No GO Terms	2	8.7	37.661
10633	PF00248	Aldo/keto reductase family	No GO Terms			
01577	PF00795	Carbon-nitrogen hydrolase	GO:0006807: Nitrogen compound metabolic process	2	8.7	37.661
02924	PF00208	Glutamate/Leucine/Phenylalanine/Valine dehydrogenase	GO:0016491: Oxidoreductase activity; GO:0006520: Cellular amino acid metabolic process; GO:0055114: Oxidation-reduction process	2	37.2	39.248

A15-ARP23 Co-culture

[a] Gene ID are preceded by >AgAr|ABP

[b] Descriptions limited to Pfam relating to main protein function. Anchoring domains, for example, are not included but can be deduced from full list of Pfams provided.

Table 2: SSDA secreted and extracellular proteins relating to carbohydrate metabolism of A15 monocultures compared to A15 co-cultures. Proteins considered; $P < 0.05$, $\log_2$ fold-change ≥ 1.5.

			A15-A15		A15-CWH		A15-ARP23	
Accession No.[a]	**Pfams**	**Description[b]**	**p-value**	**FC (log2)**	**p-value**	**FC (log2)**	**p-value**	**FC (log2)**
229390	PF00150	Cellulase (GH5)	4.47E-05	↓6.67	2.11E-05	↓6.79	1.51E-04	↓5.78
114473	PF01522	Polysaccharide deacetylase	2.96E-03	↑2.17	1.03E-04	↑2.88	2.49E-02	↑1.55
194656	PF01522	Polysaccharide deacetylase	3.05E-02	↑1.69	1.75E-02	↑2.72	np	np
195052	PF00933, PF01915, PF14310	GH3/Fibronectin type III-like	7.08E-05	↓2.08	4.50E-04	↓1.82	1.91E-04	↓2.13
194280	PF01670	GH12	2.66E-04	↓4.50	1.39E-03	↓4.06	1.50E-02	↓2.71
70106	PF17801, PF16499	Alpha galactosidase A	1.55E-05	↓6.17	2.66E-05	↓5.72	1.69E-04	↓4.67
194630	PF01263	Aldose 1-epimerase	1.21E-04	↓6.73	8.06E-03	↓3.69	5.99E-04	↓3.78
193587	PF00278	GH20	2.59E-04	↑1.51	7.98E-04	↓2.42	1.01E-03	↓2.00
217305	PF00933, PF01915, PF14310	GH3/Fibronectin	4.71E-04	↓1.61	np	np	6.52E-03	↓2.10
194297	PF00722	GH16	5.86E-04	np	np	np	2.15E-02	↑1.86
192455	PF00723, PF00686	GH15/starch binding domain	6.82E-04	↓1.89	np	np	3.33E-03	↓1.60
194940	PF00295	GH28	6.32E-04	↓5.16	np	np	9.06E-04	↓3.28

211936	PF00704	GH18	9.09E-05	↓1.78	np	np	4.52E-03	↓2.03
190944	PF01055, PF13802, PF16863	GH31/Galactose mutarotase-like	1.82E-04	↓1.88	np	np	6.85E-03	↓1.52
79914	PF00450	Serine carboxypeptidase	2.49E-03	↓1.51	2.99E-03	↓1.74	np	np
227191	PF00704	GH18	5.60E-03	↓2.66	2.70E-03	↓2.80	np	np
203798	PF17678, PF07971	GH92	3.00E-03	↓2.83	3.44E-03	↓2.71	np	np
136707	PF00734, PF01083	Fungal Cellulose binding/Cutinase	2.22E-03	↓3.42	2.63E-03	↓3.16	np	np
191333	PF16862	GH79	1.72E-02	↓3.53	3.30E-03	↓3.35	np	np
217231	PF01979	Amidohydrolase family	3.23E-04	↓2.05	2.81E-05	↓2.11	np	np
199426	PF00316	Fructose-1-6-bisphosphate	1.32E-02	↑1.82	np	np	np	np
136775	PF00704	GH18	1.42E-03	↑1.54	np	np	np	np
194179	PF01532	GH47	1.38E-02	↓1.70	np	np	np	np
64273	PF16863, PF13802, PF01055	GH31	5.24E-04	↓1.71	np	np	np	np
211936	PF00704	GH18	9.09E-05	↓1.78	np	np	np	np
194180	PF01532	GH47	np	np	2.97E-02	↑1.95	np	np
188016	PF02055	GH30	np	np	3.64E-04	↓2.64	np	np
190841	PF07470	GH88	np	np	9.74E-03	↓2.69	np	np
196213	PF00734, PF10503	Fungal cellulose binding domain/Esterase PHB	np	np	1.26E-04	↓6.32	np	np

		depolymerase						
230096	PF17678, PF07971	GH92	np	np	np	np	1.01E-02	↓3.26
133541	PF00331	GH10	np	np	np	np	1.85E-03	↓6.80
191440	PF00331	GH10	np	np	np	np	3.70E-04	↓8.97
194521	PF00840, PF00734	GH7/Fungal cellulose binding domain	np	np	np	np	1.78E-03	↓9.28
185916	PF02782, PF00370	FGGY family of carbohydrate kinases	np	np	np	np	1.55E-02	↓1.54

[a] Gene ID from JGI are preceded by >jgi|Agabi_varbisH97_2|

[b] Descriptions limited to Pfam relating to main protein function. Anchoring domains, for example, are not included but can be deduced from full list of Pfams provided.

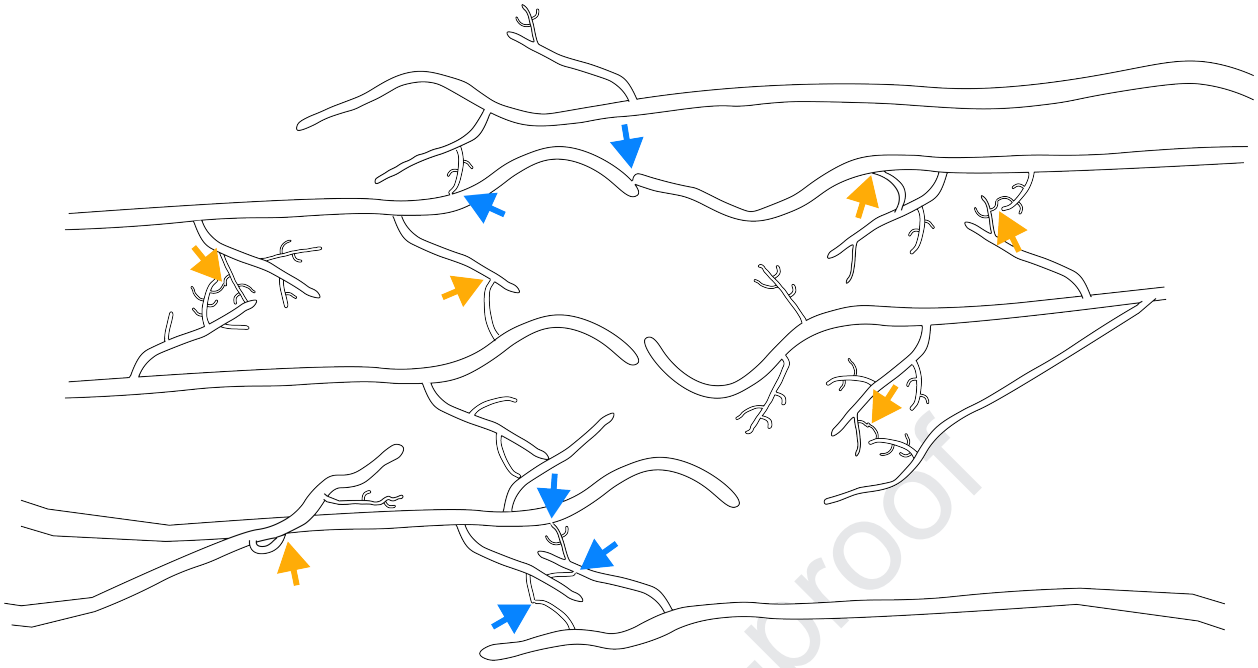

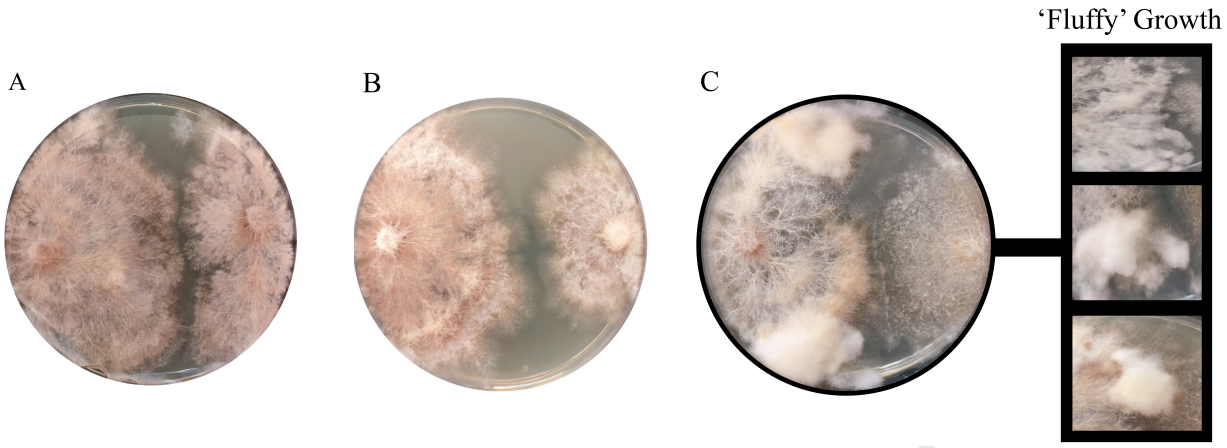

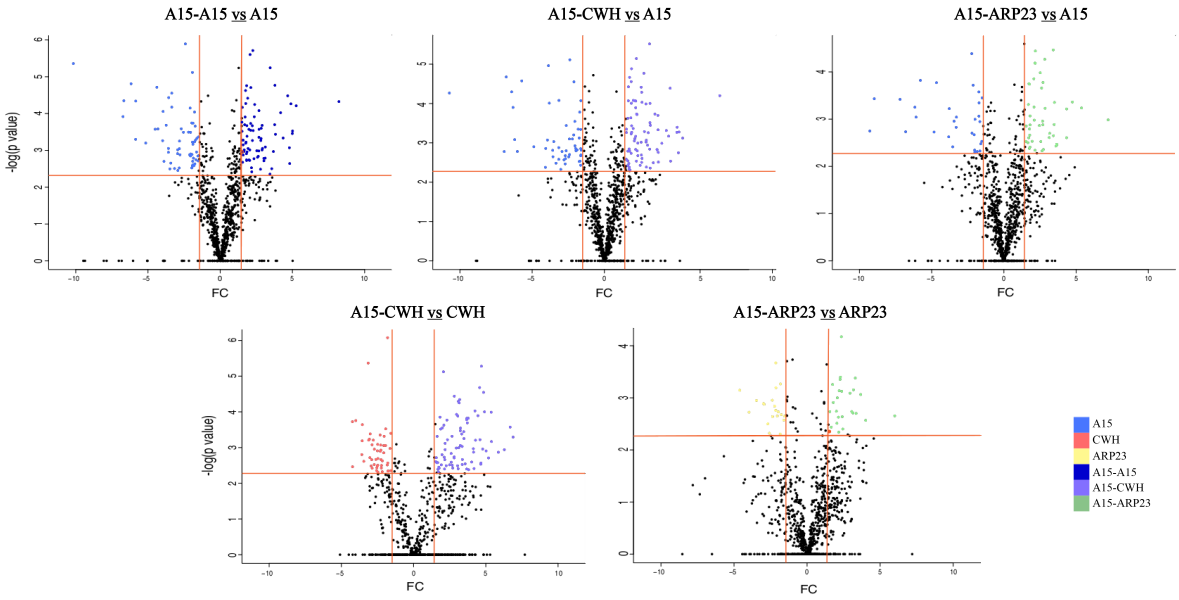

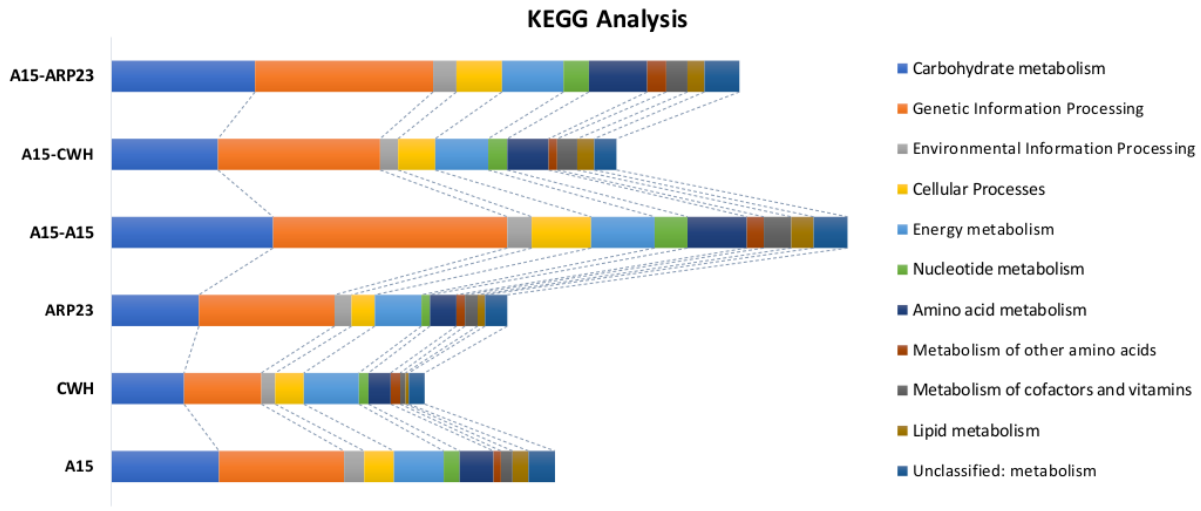

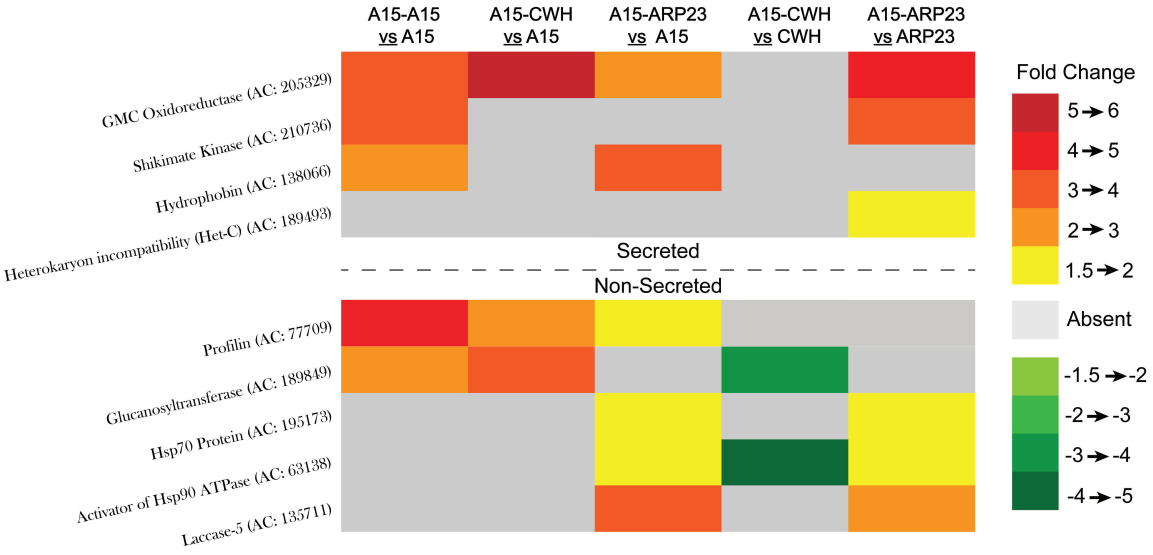
A15-A15 vs A15
A15-CWH vs A15
A15-ARP23 vs A15
A15-CWH vs CWH
A15-ARP23 vs ARP23
GMC Oxidoreductase (AC: 205329)
Shikimate Kinase (AC: 210736)
Hydrophobin (AC: 138066)
Heterokaryon incompatibility (Het-C) (AC: 189493)
Secreted
Non-Secreted
Profilin (AC: 77709)
Glucanosyltransferase (AC: 189849)
Hsp70 Protein (AC: 195173)
Activator of Hsp90 ATPase (AC: 63138)
Laccase-5 (AC: 135711)
Fold Change
5 → 6
4 → 5
3 → 4
2 → 3
1.5 → 2
Absent
-1.5 → -2
-2 → -3
-3 → -4
-4 → -5

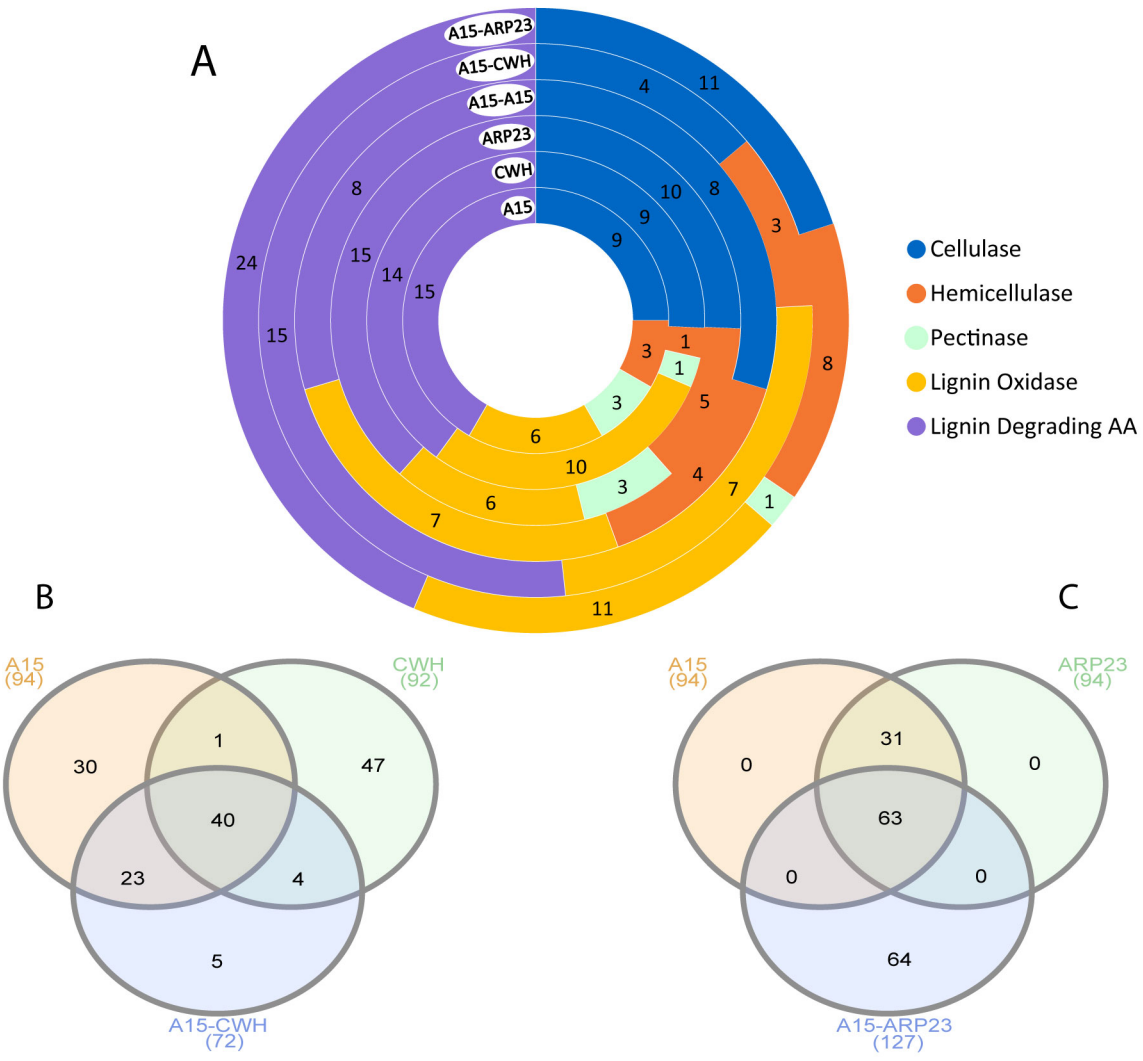
A
A15-ARP23
A15-CWH
A15-A15
ARP23
CWH
A15
Cellulase
Hemicellulase
Pectinase
Lignin Oxidase
Lignin Degrading AA
B
A15 (94)
CWH (92)
A15-CWH (72)
30
1
47
40
23
4
5
C
A15 (94)
ARP23 (94)
A15-ARP23 (127)
0
31
0
63
0
0
64

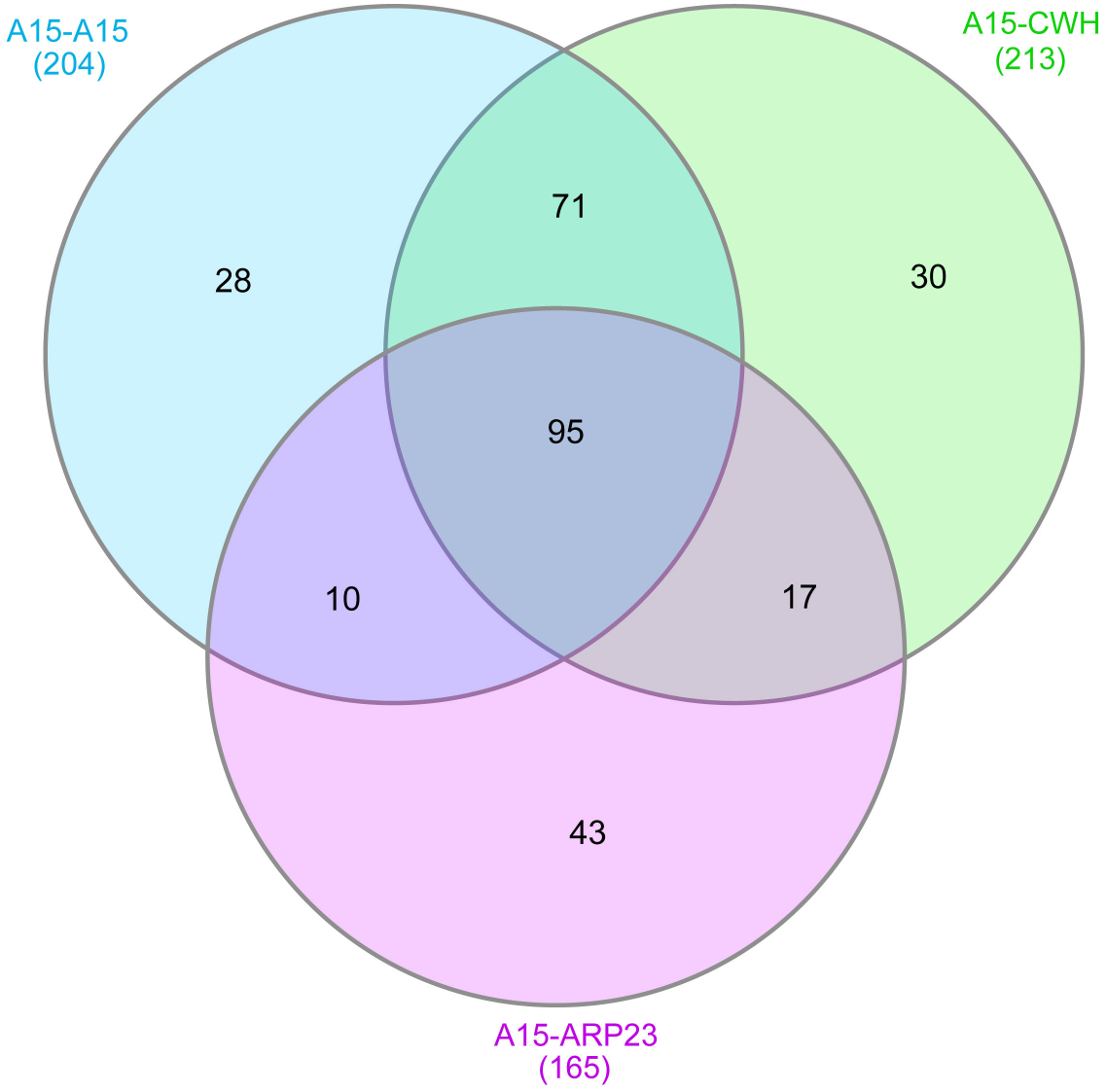
A15-A15
(204)
A15-CWH
(213)
A15-ARP23
(165)
28
71
30
95
10
17
43

Highlights

- Unique proteomic responses detected between all *A. bisporus* strain co-cultures.
- Cell wall, fungal growth and morphogenesis proteins are differentially abundant.
- Nitrogen starvation evident between competing and non-compatible strains.
- Carbohydrate-active enzymes are expanded in antagonistic *A. bisporus* interactions.